CAPITAL UNIVERSITY OF SCIENCE AND
TECHNOLOGY, ISLAMABAD

Attenuation of Acoustic Waves from Wiremesh Interfaces

by

Armghan Ahmed

A thesis submitted in partial fulfillment for the
degree of Master of Philosophy

in the

Faculty of Computing
Department of Mathematics

2025

*I dedicate my dissertation work to my **family** and dignified **teachers**. A special feeling of gratitude to my loving parents who have supported me in my studies.*

CERTIFICATE OF APPROVAL

Attenuation of Acoustic Waves from Wiremesh Interfaces

by

Armghan Ahmed

(MMT221012)

THESIS EXAMINING COMMITTEE

S. No.	Examiner	Name	Organization
(a)	External Examiner	Dr. Amer Bilal Mann	FUUAST, Islamabad
(b)	Internal Examiner	Dr. Dur e Shehwar	CUST, Islamabad
(c)	Supervisor	Dr. Abdul Rehman Kashif	CUST, Islamabad

Dr Abdul Rehman Kashif
Thesis Supervisor
September, 2025

Dr. Muhammad Sagheer
Head
Dept. of Mathematics
September, 2025

Dr. M Abdul Qadir
Dean
Faculty of Computing
September, 2025

Author's Declaration

I, **Armghan Ahmed**, hereby state that my MPhil thesis titled "**Attenuation of Acoustic Waves from Wiremesh Interfaces** " is my work and has not been submitted previously by me for taking any degree from Capital University of Science and Technology, Islamabad or anywhere else in the country/abroad.

At any time if my statement is found to be incorrect even after my graduation, the University has the right to withdraw my MPhil Degree.

(Armghan Ahmed)

Registration No: MMT221012

Plagiarism Undertaking

I solemnly declare that the research work presented in this thesis is titled "**Attenuation of Acoustic Waves from Wiremesh Interfaces**" is solely my research work with no significant contribution from any other person. Small contribution/help wherever taken has been dully acknowledged and that complete thesis has been written by me.

I understand the zero tolerance policy of the HEC and Capital University of Science and Technology towards plagiarism. Therefore, I as an author of the above-titled thesis declare that no portion of my thesis has been plagiarized and any material used as reference is properly referred/cited.

I undertake that if I am found guilty of any formal plagiarism in the above-titled thesis even after awarded of MPhil Degree, the University reserves the right to withdraw/revoke my MPhil degree and that HEC and the University have the right to publish my name on the HEC/University website on which names of students are placed who submitted plagiarized work.

(Armghan Ahmed)

Registration No: MMT221012

Acknowledgement

I got no words to articulate my cordial sense of gratitude to **Almighty Allah** who is the most merciful and most beneficent to his creation.

I also express my gratitude to the last prophet of **Almighty Allah, Prophet Muhammad (PBUH)** the supreme reformer of the world and knowledge for a human being.

I would like to be thankful to all those who provided support and encouraged me during this work.

I would like to be grateful to my thesis supervisor **Dr. Abdul Rehman Kahif**, for guiding and encouraging me in writing this thesis. It would have remained incomplete without his endeavours. Due to his efforts, I was able to write and complete this assertation.

I would like to express my deepest gratitude to my most respectable professor, **Dr. Muhammad Afzal**, for his invaluable guidance, encouragement, and support throughout the course of this research. His insightful suggestions, patience, and constant motivation have been instrumental in helping me to complete this thesis. I am truly grateful for the time and effort he dedicated to mentoring me, and for always inspiring me to strive for excellence in my work. I also would like to pay great tribute to my **parents**, and my **wife** for their prayers, moral support, encouragement and appreciation.

Last but not the least, I want to express my gratitude to my **friends** who helped me throughout my MPhil degree.

(Armghan Ahmed)

Abstract

The primary objective of this study is to model and analyze wave scattering in a rectangular waveguide equipped with either a single or double wire mesh. Two configurations are examined: one involving a single wire mesh, and the other featuring a double wire mesh within the waveguide. The associated boundary value problem is solved using the separation of variables technique. This analytical method involves representing the wave field as a series expansion of the waveguide's eigenmodes and applying boundary condition matching at the interfaces to compute the mode coefficients. The study particularly focuses on employing the separation of variables approach to evaluate the wave scattering behavior, velocity, pressure and frequency. Understanding this behavior is important for various applications in structural acoustics as well as in heating, ventilation, and air-conditioning (HVAC) systems. This work investigates how local losses caused by a resistive wire mesh influence the modes of an acoustic cavity. In the one dimensional case, we show that the wire mesh can selectively affect the modes ranging from leaving them completely unchanged to fully absorbing them. This property can be exploited to filter cavity modes. In the two dimensional case, we extend the analysis to higher-order modes and examine how tilting the wire mesh impacts the cavity modes. Notably, we identify a new type of mode that is localized on the wire mesh and characterized by a purely imaginary eigenfrequency. Also in a two dimensional rectangular waveguide, a double wire mesh is used with soft and rigid boundary conditions to analyze the velocity and pressure profiles of a scattered wave.

Contents

List of Figures

Abbreviations

BVP	Boundary Value Problem
HVAC	Heating, Ventilation and Air-Conditioning
MM	Mode-Matching
ODEs	Ordinary Differential Equations
PDEs	Partial Differential Equations

Symbols

c	Speed of sound
C_p	Constant pressure
k	Wave number
u	Flow velocity
τ	Stress tensor
α	Transverse wavenumber
g	Gravitational acceleration
p	Instantaneous pressure
p_0	Equilibrium pressure
T	Temperature
ω	Angular frequency
∇	Divergence
∇_p	Exerting force
β	Bulk modulus
Φ	Fluid velocity potential
$\hat{Z}$	Impedance
η_n	axial wavenumber
δ_{mn}	Kronecker delta
$\sum$	Summation
ρ_0	Density of air

Chapter 1

Introduction and Background Survey

Acoustic is the branch of physics that deals with the study of pressure fluctuations in gasses, solids and liquids, such as vibration. In prehistoric times, acoustics played a vital role in managing sound within structures like stadiums, places of worship, and concert halls. However, in the modern era, the scope of acoustics extends far beyond noise control and finds applications across all fields of science. It has been categorized into various branches, including medical acoustics, architectural acoustics, physical and engineering acoustics, musical acoustics, and others.

Acoustics is applied in various noise reduction challenges, such as: (i) Architectural noise issues; noise which produced in duct of heating and ventilation system, (ii) Noise issues in aerodynamic; propagation of noise in wind tunnels, (iii) In road transportation; exhaust noise from internal combustion engine and (iv) Construction and Industrial noise; machinery, factories and building sites. Noise typically propagates through ducts or pipes. The design of these ducts and pipes plays a crucial role in reducing noise. As they serve as primary channels for energy transmission from one point to another. Moreover for the noise of Heating Ventilation and Air Conditioning (HVAC) system of buildings, different duct designs and sound proofing are used. It works like a channel which transports vibrational

energy from one point of the medium to another point. The investigation on designs and materials properties of such ducts in order to minimize the vibrational energy has gained much attention of researchers and engineers. The current study is relevant for the propagation and attenuation of sound waves in a waveguide that includes porous material and wire mesh. The material properties of the absorptive material can be varied. Such waveguides may have application in HVAC and silencer designs. The current study is about the forces on the modeling of acoustic waves their propagation, scattering, and absorption.

1.1 Literature Review

An acoustic rectangular waveguide is a structure that directs sound waves within a rectangular cross-section, commonly used in duct acoustics, ultrasonic wave propagation, and musical instruments. It confines sound waves between rigid walls, allowing only specific wave patterns, called modes, to propagate. The behavior of these waves is governed by the wave equation, which determines how the sound pressure varies within the waveguide. Each mode has a cut-off frequency, meaning that it only propagates if the sound frequency is high enough, otherwise the wave decays. The fundamental mode travels without distortion, while higher-order modes introduce complex variations in pressure. These waveguides exhibit dispersion, where the wave speed depends on the frequency, which affects the way sound travels. Their ability to control sound waves makes them essential in applications such as ventilation ducts, ultrasound devices, and resonance chambers in musical instruments [1]. Rectangular acoustic waveguides play a crucial role in modern life, shaping that's, how sound is transmitted and controlled in various applications. They are used in HVAC duct systems to guide airflow while minimizing noise, ensuring quieter and more efficient buildings. In ultrasound technology, these waveguides help focus and direct sound waves for medical imaging and industrial inspections. They are also essential in loudspeakers and musical instruments, where they enhance sound projection and resonance. In aerospace and automotive industries, they help reduce engine noise and improve cabin acoustics. Even in communication systems, such as underwater sonar, they enable precise

sound transmission. By controlling how sound waves travel, rectangular acoustic waveguides improve comfort, efficiency, and technology in everyday life.

An acoustic rectangular waveguide with wire mesh is a specialized structure designed to control and direct sound waves while allowing airflow. These waveguides consist of rigid rectangular ducts that are similar to a standard acoustic waveguide but with a wire mesh integrated into its structure. The wire mesh acts as a partially transparent acoustic barrier, allowing some sound to pass through while reflecting or attenuating certain frequencies. This design is commonly used in ventilation systems, exhaust ducts, and noise control applications, where it helps to manage sound transmission while maintaining airflow.

The mesh can be tuned to specific acoustic properties by adjusting its pore size, material, and thickness, allowing it to selectively filter unwanted noise while allowing necessary sounds or air to pass through. In ultrasonic applications, wire mesh waveguides can also help shape and guide high-frequency waves for precise industrial or medical uses. This combination of structural rigidity and acoustic filtering makes wire mesh waveguides a valuable tool in both engineering and noise management [2].

The use of wire mesh in acoustics has a rich history that spans industrial applications, architectural design, and advanced scientific research. Its development as a tool for manipulating acoustic waves began in the early 20th century, primarily in industrial settings where engineers needed materials that could reduce noise while maintaining airflow. Wire mesh was initially employed in ventilation systems, mufflers, and machinery enclosures because of its ability to attenuate high-frequency noise through reflection and scattering while allowing air to pass through.

This made it ideal for applications such as exhaust systems and factory noise barriers, where solid walls would impede ventilation. By the mid-20th century, researchers began systematically studying how wire mesh interacted with sound waves. Scientists explored its acoustic impedance, porosity, and damping properties, leading to a better understanding of how the geometry of mesh (wire thickness, spacing, and open area ratio) influenced sound absorption and transmission. The

wire mesh also in controlling and manipulating electromagnetic (EM) waves dates back to the late 19th and early 20th centuries, closely tied to the development of radio technology, shielding methods and microwave engineering. Its ability to interact with EM fields either by reflecting, transmitting, or filtering specific frequencies has made it indispensable in various scientific, military, and industrial applications.

The foundational principle behind wire mesh in EM applications stems from Michael Faraday's work on electrostatic shielding in the 1830s. Faraday demonstrated that a conductive enclosure could block external electric fields. Wire mesh, being a lightweight and flexible conductive material, became a practical implementation of this concept [3]. By the early 1900s, as radio technology advanced, engineers used wire mesh to construct shielded rooms to prevent interference in sensitive radio communications.

The mesh acted as a high-pass filter, blocking the lower frequency electrostatic fields while allowing higher frequency radio waves to pass if the openings were sufficiently large compared to the wavelength. From Faraday cages to 5G antennas and metamaterials, wire mesh has been a fundamental tool in controlling electromagnetic waves for over a century. Its unique combination of conductivity, flexibility, and tunable filtering properties ensures its continued relevance in both traditional shielding applications and cutting-edge EM wave engineering.

Acoustic rectangular waveguides with wire mesh have several practical applications, particularly in noise control, ventilation systems, and ultrasonic technology. In automotive and aerospace engineering, these waveguides are used in mufflers and jet engine ducts to dampen engine noise while maintaining airflow. In ultrasonic applications, such as medical imaging and industrial non-destructive testing, wire mesh waveguides help direct and shape high-frequency sound waves, improving precision and efficiency. Additionally in architectural acoustics, they are used in noise barriers and soundproofing designs to absorb and diffuse sound in auditoriums, concert halls, and recording studios. By combining sound control with airflow management, these waveguides provide a versatile solution for various engineering and acoustic challenges. In architectural acoustics, they are used in soundproofing

panels, noise barriers, and concert hall designs to control how sound travels within a space.

The wire mesh can help diffuse or absorb sound at specific frequencies, improving the clarity and quality of speech or music in auditoriums and recording studios. Overalls acoustic rectangular waveguides with wire mesh offer a unique combination of sound control and airflow management, making them essential in industries where both noise reduction and ventilation are required. Their ability to be tailored for specific frequencies and applications ensures they play a critical role in engineering, transportation, healthcare, and building acoustics.

However, advancements in material science, metamaterials, and smart acoustics are opening new frontiers for its use in manipulating sound waves. In the coming decades, wire mesh is expected to revolutionize ultrasonic imaging, active noise cancellation, acoustic cloaking, and even quantum acoustics. Wire mesh plays a multifaceted and critical role in quantum acoustics, where it functions as a key component in controlling, manipulating, and enhancing phononic interactions at the quantum level. Furthermore, wire mesh can serve as an acoustic metamaterial, enabling unconventional phonon manipulation, such as negative refraction or topological phononics, which are crucial for advancing quantum simulations and information processing.

In experimental setups, wire mesh structures often fabricated from metals or superconductors are used to engineer phononic bandgaps, analogous to photonic crystals in optics, by creating periodic variations in acoustic impedance. These bandgaps allow researchers to selectively block or transmit specific phonon frequencies, enabling precise control over surface acoustic waves (SAWs) and bulk acoustic waves in piezoelectric substrates. Such control is essential for developing quantum acoustic devices, including phononic waveguides, resonators, and transducers that interface mechanical motion with superconducting quantum bits or optical photons [4].

In the 20th century, Sabine, known as the father of architectural acoustics, measured the amount of sound within rooms and designed acoustically optimized theaters. Rayleigh developed a method for measuring the intensity of a sound source.

Knudsen and Harris built upon Sabine's work by studying the impact of molecular relaxation phenomena in gases and liquids. With the assistance of Beranek and Newman, Bolt contributed to the design and development of acoustical buildings, concert halls, music pavilions, and performing arts centers. Lighthill conducted research on nonlinear acoustics in fluids. Hamilton, Blackstock, and Beyer explored the propagation of sound through liquids, gases, and solids [5].

The present study is related to the propagation and scattering of acoustic waves in rectangular waveguide or channel wire-mesh condition. The performance of acoustical waveguide to reduce unwanted noise can be increased by using the noise absorbent material and introducing the locally reactive liners. The salient features of acoustic scattering in guiding structures that contain expansions and/or contraction in geometry have vital role in noise reduction applications.

The propagation of wave along the ducts with rapid changes in the cross sectional area can produce reaction that reduce the energy of transmitted wave. Norton and Werby [6] discussed the numerical technique to describe acoustical scattering and propagation from an object in a waveguide. Tielbürger et al. [7] explained the acoustic propagation through an internal wave field in a shallow water waveguide. Cai et al. [8] described the acoustical scattering by arrays of cylinders in waveguides. Maurel et al. [9] are concerned with the wave propagation through penetrable scatterers in a waveguide and through a penetrable grating. Plamenevskii and Poretskii [10] considered the mathematical scattering theory in quantum and acoustic waveguides. Modeling the sound propagation in acoustic waveguides using a hybrid numerical method by Kirby [11].

Lawrie [12] tells the mode-matching technique to analysis the mode-matching for acoustic scattering in three dimensional waveguides with flexible walls. The significant ability of porous media to absorb and modify incident sound waves, due to their interaction with the fluid within the pores, has generated considerable interest in their acoustic behavior. Afsara and Alam [13] worked on mode-matching analysis of flexural trifurcated waveguide with porosity effects. Exceptional points (which occur when two or more modes coalesce) have long been associated with optimal attenuation in lined acoustic waveguides. The analytic mode-matching for

accurate handling of exceptional points in a lined acoustic waveguide explained by Lawrie et al. [14]. Muehleisen and Swanson [15] discussed modal coupling in acoustic waveguides.

The propagation of sound waves in an infinite circular cylindrical pipe with an inserted perforated screen is investigated rigorously through the mode matching technique. Tiryakioglu [16] used mode matching technique to analysis of sound waves in an Infinite pipe with perforated screen. On the extension of the mode-matching procedure for modeling a wave-bearing cavity explained by Bilal and Afzal [17].

Lawrie and Afzal [18] are concerned with the reflection and transmission of fluid-structure coupled waves at the junction between two flexible waveguides of different heights. Using the eigenmodes of the silencer in an analytic mode matching approach, Cummings and Chang [19] enforced continuity of pressures and velocities in the inlet and outflow planes of the silencer. Nennig et al. [20] discussed a mode matching approach for modeling two dimensional porous grating with infinitely rigid or soft inclusions. Lawrie and Kirby [21] discussed a point collocation approach to modelling large dissipative silencers.

Accordingly, the dispersion of waves through different layered medium is discussed in [22]. The present work is in continuation of the aforementioned studies with expansion chamber containing sound absorbent material along with backward propagation. Recently Haung [23] and then Haung and Choy [24] investigated different aspects of channels for distortion of fan noise in HVAC system.

Lawrie [25] presented the class of orthogonality relations relevant to fluid-structure interaction. Haung [26] analyzed drum like silencer and reflection of sound waves through chamber enclosed by vertical plates. The present work is geometrical extended form of the work done by Demir and Buyukaksoy [27]. In 1999, Iserles et al. [28] made a study on the solution of linear differential equation using Lie groups and investigated the solution of the first order linear homogenous differential equation $x' = H(t)x$. In 2006, Cases and Iserles [29] examined and introduced the algorithim for nonlinear differential equation. Magnus series have taken attention in the theory of differential equation [30] and control theory [31]. The study

in continuation of the work carried by Pagneux [32] with addition to soft-soft and rigid-soft settings. Felix [33] assumed adiabatic lossy medium lined with reacting liners. The propagation of sound waves in lined ducts having rigid walls have been discussed by many authors, for instance see [34, 35]. Surface and interface acoustic waves are two-dimensionally guided waves, as their displacement field is plane-wave like regarding its dependence on the spatial coordinates parallel to the guiding plane, while it decays exponentially along the axis normal to that plane. When propagating at the planar surface or interface of homogeneous media, they are non-dispersive. Another type of non-dispersive acoustic waves which is, however, one-dimensionally guided, has displacement fields localized near the apex of a wedge made of an elastic material. In this short review, their propagation properties are described as well as theoretical and experimental methods which have been used for their analysis by Mayer et al. [36].

Groth et al. [37] investigated the propagation of elastic waves in rectangular waveguide structures to determine dispersion curves and explore their applications in nondestructive testing (NDT). The use of mechanical waves for evaluating structural integrity is a well-established NDT method. However, when using ultrasound in the form of guided waves, a deep understanding of the complex propagation behavior is essential for developing advanced damage detection techniques. In this context, understanding how wave propagation interacts with the geometry of the waveguide becomes crucial. Zhang et al. [2] presented a mechanistic analysis and experimental study of wire mesh-assisted ventilated acoustic metamaterials, utilizing both an analytical acoustic model and a numerical acoustic-flow coupling model. Kuznetsova et al. [38] studied about Higher-order mode filtering by a resistive layer. A method for filtering higher-order acoustic modes using a resistive layer is proposed and applied to a two-dimensional rectangular waveguide with a quiescent fluid. An analogue of Cremer's criterion is discussed and used to obtain the optimal modal attenuation of the non-planar waves while the plane wave is preserved. Yanhong et al. [39] investigate the experimental study on the wave propagation characteristics of entangled metallic wire materials using acoustic emission techniques. A wire mesh liner exhibits better acoustic linearity under high sound pressure levels (SPL) compared to a perforated liner; however, it

lacks a precise impedance model. Therefore, this study investigates its nonlinear behavior at high SPL. A jet flow simulation through mesh openings—modeled as two-dimensional slits—is performed. The results show that the nonlinear loss approximation in existing models implicitly includes linear losses and overlooks the influence of uniform orifice distribution. As a result, the nonlinearity of distributed micro-orifices tends to be overestimated. Qiu et al. [40] presented nonlinear effect of wire mesh liners subjected to high sound pressure level. Four types of boundary conditions Dirichlet, Neumann, transmitting, and modified transmitting—are derived by integrating the damped wave equation with their respective boundary formulations. Among them, the Dirichlet attenuating boundary condition is the simplest to implement. With a suitable choice of attenuation parameter, it can reduce boundary reflections to just a few percent within a zone approximately one wavelength wide. The Neumann attenuating condition behaves similarly but is more complex to implement numerically. Both the transmitting and modified transmitting boundary conditions require an absorbing boundary at the end of the attenuating region. The modified transmitting condition is the most effective in minimizing boundary reflections. In multidimensional simulations, perfect absorbing boundaries do not exist, so approximate absorbing boundary conditions are employed instead. Gal et al. [41] discussed the oscillatory boundary conditions for acoustic wave equations.

The sound field generated by a point source near the interface between two media cannot be accurately determined using the acoustic-ray approach. This method, which relies on reflection coefficients for plane waves, yields inconsistent and incorrect results, particularly at grazing incidence. This analytical approach is applied to the case of an acoustic point source, and the resulting findings are presented. Rudnick [42] explained the propagation of an acoustic wave along a boundary. By decomposing the acoustic wave equation into incoming and outgoing components, an absorbing boundary condition can be formulated to suppress reflections of plane waves based on their propagation direction. This condition is defined by a first order differential operator, known as the absorbing boundary operator, which serves as the fundamental building block for constructing more advanced boundary conditions. These operators can be specifically designed to perfectly absorb

plane waves traveling in one or two directions. By combining multiple absorbing operators, boundary conditions can be tailored to absorb waves propagating in several directions. This approach greatly simplifies the design of boundary conditions aimed at minimizing the adverse effects of outgoing waves in various wave propagation scenarios. Keys [43] investigated the absorbing boundary conditions for acoustic media.

Takekawa and Mikada [44] developed an absorbing boundary condition for acoustic wave propagation that maintains the flexibility of mesh-free methods. In numerical simulations, it is crucial to eliminate artificial reflections at model boundaries caused by the truncation of the computational domain. While many absorbing boundary conditions exist, most are designed for regularly aligned grids or nodes, and their effectiveness for irregular configurations has not been thoroughly evaluated. To address this, the authors examined artificial reflections occurring at the boundaries in mesh-free simulations and proposed a novel technique to suppress these artifacts. Their method employs a hybrid approach with a transition zone, where the wave field is computed as a weighted average of solutions from both one-way and two-way wave equations. Numerical results demonstrate that this approach effectively reduces artificial edge reflections, even in cases where the distribution of computational points near the boundaries is irregular.

In the theory of mechanics and mathematical physics involving prismatic domains, the method of separation of variables typically results in Sturm Liouville type eigenproblems associated with self-adjoint operators, enabling the use of eigenfunction expansions to solve the equations. However, many significant practical problems do not yield self-adjoint operators in the transverse coordinate. To address this, a generalized variational principle is derived from the principle of minimum potential energy by appropriately selecting the state variables and their corresponding dual variables. Wanxie and Xiangxiang [45] discussed method of separation of variables and Hamiltonian system.

In this dissertation we will discuss acoustic rectangular waveguide with single and double wire mesh in which a structure designed to control sound propagation while allowing airflow. In a single wire mesh configuration, a single layer of mesh

is placed within the waveguide, acting as a semi transparent acoustic barrier that partially reflects, absorbs, or transmits sound waves depending on the frequency. In contrast, a double wire mesh configuration features two layers of mesh, which can be arranged at different positions or with varying spacing inside the waveguide. This design enhances sound attenuation and frequency filtering by creating interference effects that further reduce noise transmission. Double mesh structures are often used in high-performance noise reduction systems, ultrasonic applications, and industrial soundproofing, where precise control over sound wave behavior is required.

The choice between single and double wire mesh depends on the desired level of noise reduction, airflow requirements, and specific application needs, making these waveguides versatile tools in engineering, architecture, and industrial acoustics.

For example, in factories and power plants, where large machines generate significant noise, double mesh waveguides inside exhaust vents or cooling systems help absorb and reflect more sound waves, preventing excessive noise from spreading into the workplace. Another practical use of double wire mesh waveguides is in ultrasound and non-destructive testing.

1.2 Thesis Contribution

In the present study, which is motivated by the aforementioned literature review, we aim to describe the characteristics of acoustic wave in rectangular waveguide with wire mesh conditions.

1.3 Thesis Layout

This dissertation is divided into the following five chapters. **Chapter 1** provide an introduction to the topic, discuss its historical context, and review relevant literature. **Chapter 2** demonstrates some important definitions, laws, and concepts which are useful to understand the next work. [10pt] **Chapter 3** contains

the propagation of acoustic waves through an infinite and semi-infinite rectangular waveguide with single wire mesh and rigid boundary condition. **Chapter 4** includes three regions with wire double mesh and also including soft and rigid boundary condition boundary conditions. [10pt] **Chapter 5** provides the summary and concluding remarks of the thesis. References used in the thesis are mentioned in **Bibliography**.

Chapter 2

Preliminaries

This chapter contains some basic definitions and governing laws, which will be helpful in the subsequent chapters.

2.1 Wave

Wave is the disturbance in the medium which causes the particles of that medium to vibrate from one place to another to transfer the energy. It is important to know that waves transfer energy of the matter without transferring matter. Typical examples include light waves and sound waves etc [46].

2.2 Types of Waves

There are three types of waves based on the medium characteristics and energy propagation [46]. These includes:

1. Mechanical waves
2. Electromagnetic waves
3. Matter waves

2.2.1 Mechanical Waves

Mechanical waves are the type of waves in which energy is transferred through the oscillations produced in a material medium. Waves produced on the strings and springs are some common examples.

2.2.2 Electromagnetic Waves

The waves which are created when electric and magnetic fields oscillate perpendicular to each other are known as electromagnetic waves. These are the only waves that do not need any material medium for the transfer of energy. These waves travel in a vacuum with the same speed. The X rays, microwaves and radio waves are some common examples of electromagnetic waves.

2.2.3 Matter Waves

Light has both the natures, sometimes it act as radiation and sometimes it acts as material which has momentum and which can strike with a force. The dual nature of light to exist as both material and in wave form is known as matter waves.

2.3 Waveguides

Waveguides are structures engineered to direct waves such as sound or electromagnetic waves by limiting their spread to one or two dimensions, thereby reducing energy loss. Their shape and design dictate their function, and in acoustics, waveguides operate similarly to transmission lines, enabling efficient sound wave propagation within them [47].

2.4 Properties of Waves

For further explanation about waves, it is appropriate to know about basic properties of waves [48].

2.4.1 Amplitude

Amplitude in a wave refers to the maximum displacement or variation of a wave from its equilibrium or rest position. It is a measure of the wave's strength or intensity. In mechanical waves, such as sound waves traveling through air, the amplitude represents the maximum displacement of air particles from their normal positions.

For pressure waves, amplitude corresponds to the maximum variation in pressure from the ambient level. A larger amplitude means a more energetic wave, and in the context of sound, it translates to a louder perceived sound.

2.4.2 Frequency

In wave motion, frequency refers to how many complete wave cycles pass a given point in one second. It is denoted by f and measured in hertz (Hz). Frequency reflects how rapidly the wave oscillates in time. A higher frequency means more oscillations per second, which usually corresponds to a higher-pitched sound in acoustics or a higher-energy wave in physics. The wave number denoted by k, represents how many wave cycles fit into a unit distance and is defined as $k = \frac{2\pi}{\lambda}$, where λ is the wavelength. The wave number measures the spatial variation of the wave, while frequency measures the temporal variation. Both are connected through the wave speed c by the relation:

$$k = \frac{2\pi f}{c}, \tag{2.1}$$

or equivalently,

$$f = \frac{ck}{2\pi}. \tag{2.2}$$

2.4.3 Time Period

The time period of a wave is the amount of time it takes for one complete cycle of the wave to pass a fixed point. It is denoted by the symbol T and is typically

measured in seconds. The time period is the reciprocal of the wave's frequency, meaning $T = \frac{1}{f}$, where f is the frequency in hertz Hz.

2.4.4 Crest

The crest is the highest point of the wave particles in a medium from the mean position.

2.4.5 Trough

The lowest point of the vibrating body particles from the mean position is called a trough.

2.4.6 Wavelength

Wavelength is the distance between two identical points in consecutive cycles of a wave, such as from crest to crest or trough to trough in a transverse wave, or from compression to compression or rarefaction to rarefaction in a longitudinal wave.

In a transverse wave, particles of the medium move perpendicularly to the direction of wave propagation like waves on a string or water surface, so the wavelength is the horizontal distance between two successive crests or troughs.

In contrast, a longitudinal wave involves particle motion parallel to the direction of wave travel like sound waves in air, so the wavelength is the distance between two regions of maximum compression or maximum rarefaction in the medium. In both types of waves, the wavelength (λ) is related to the wave's speed (c) and frequency (f) by the equation:

$$\lambda = \frac{c}{f}. \tag{2.3}$$

This means that for a given wave speed, a higher frequency results in a shorter wavelength.

2.5 Acoustic Wave Equation

Acoustic wave propagation can be analyzed using differential equations, which are derived from the properties of the material medium involved, such as solid, liquid, or gas. When deriving the wave equation in a gas medium like air, the conservation laws typically result in nonlinear equations. However, discussing nonlinear wave equations can be challenging, so linear approximation theory is often employed for practicality.

In this approach, we focus on deriving the linear form of the wave equation to simplify analysis. The acoustic wave equation for sound pressure describes how pressure disturbances (sound waves) propagate through a compressible medium such as air or water [49]. The standard form of 1-Dimensional acoustic wave equation is

$$\frac{\partial^2 \Phi(x,t)}{\partial x^2} = \frac{1}{c^2}\frac{\partial^2 \Phi(x,t)}{\partial t^2}. \tag{2.4}$$

2.5.1 Helmholtz Wave Equation

The wave equation and the Helmholtz equation are closely related, and the Helmholtz equation can be derived from the wave equation under certain assumptions. The Helmholtz equation is a partial differential equation (PDE) that describes the behavior of waves in various physical systems. It's named after Hermann von Helmholtz, a German physicist and mathematician.

The Helmholtz equation is typically written as:

$$\nabla^2 \Phi + k^2 \Phi = 0. \tag{2.5}$$

The Helmholtz equation is used to model various wave phenomena, such as acoustic waves (sound waves), electromagnetic waves (light, radio waves, etc.), Water waves and Seismic waves. It's a fundamental equation in many fields, including

physics, engineering, and mathematics. The solutions to the Helmholtz equation describe the spatial distribution of waves in a given system, which is crucial for understanding and predicting wave behavior. The Helmholtz equation is often solved using various mathematical techniques, such as separation of variables, Green's functions, or numerical methods.

The wave equation describes the propagation of waves in a medium:

$$\frac{\partial^2 \Phi}{\partial t^2} = c^2 \nabla^2 \Phi. \tag{2.6}$$

We assume that $\Phi(x, y, z, t)$ can be written as the time harmonic dependent:

$$\Phi(x, y, z, t) = \Phi(x, y, z) e^{-i\omega t}. \tag{2.7}$$

Substituting (2.7) into (2.6), we get

$$\frac{\partial^2}{\partial t^2} \Phi(x, y, z) e^{-i\omega t} = c^2 \nabla^2 \Phi(x, y, z) e^{-i\omega t}. \tag{2.8}$$

Simplifying the left-hand side, we get:

$$-\omega^2 \Phi(x, y, z) e^{-i\omega t} = c^2 \nabla^2 \Phi(x, y, z) e^{-i\omega t}. \tag{2.9}$$

Rearranging the equation (2.9), we get:

$$\nabla^2 \Phi(x, y, z) + \frac{\omega^2}{c^2} \Phi(x, y, z) = 0. \tag{2.10}$$

The wave number k is

$$k = \frac{\omega}{c}. \tag{2.11}$$

Using equation (2.11) in (2.10), we obtain:

$$\nabla^2 \Phi(x, y, z) + k^2 \Phi(x, y, z) = 0. \tag{2.12}$$

This is the Helmholtz equation, which describes the spatial distribution of waves in a medium.

2.6 Boundary Conditions

The following boundary conditions are specified to formulate the boundary value problem (BVP) [50]:

1. Soft conditions
2. Rigid conditions
3. Impedance conditions
4. Edge conditions
5. Spring-like conditions
6. Fixed conditions
7. Free conditions

2.6.1 Soft Conditions

The soft boundary conditions are Drichlet's type boundary conditions. In these type of conditions, the pressure or displacement is considered as zero, i.e.

$$\psi(x, y) = 0.$$

2.6.2 Rigid Conditions

Neumann's type boundary conditions are actually rigid boundary conditions. In rigid conditions, normal velocity is considered as zero, i.e.

$$\frac{\partial \psi}{\partial x} = 0.$$

2.6.3 Edge Conditions

Edge conditions in a waveguide are the boundaries or constraints imposed on the wave field at the edges, determining how the wave behaves, such as reflection, absorption, or transmission. Common edge conditions include hard wall, soft wall, periodic, absorbing, and impedance boundaries.

2.6.4 Impedance Conditions

The impedance boundary conditions are Robin's type boundary conditions. Robin boundary conditions are mixture of Drichlet boundary conditions and Neumann boundary conditions. These conditions are written as

$$\beta_1\psi(x,y) + \beta_2\frac{\partial\psi(x,y)}{\partial x} = 0,$$

where β_1 and β_2 are arbitrary constants.

2.6.5 Spring-like Conditions

In a waveguide, spring-like conditions, also known as elastic boundaries or resilient supports, refer to boundaries where the displacement is resisted by a restoring force proportional to the displacement. These conditions simulate the behavior of a spring, allowing limited movement while exerting a force that tends to return the system to its equilibrium position.

2.6.6 Fixed Conditions

In a waveguide, a fixed condition also referred to as a "fixed boundary" or "clamped boundary" is a type of boundary where:

- The displacement (movement) is zero
- The wavefield is not allowed to move or vibrate
- The boundary is rigid and immovable

2.6.7 Free Conditions

Free conditions, also known as free boundaries, describe points in a waveguide where no external force or constraint is applied. At these boundaries, both the

bending moment and shear force are zero, allowing the structure to move and deform freely without resistance.

2.7 Strum-Liouville Equation

The Sturm–Liouville equation arises in solving many physical systems governed by partial differential equations (PDEs), especially when applying separation of variables [51].

It's a type of second-order linear differential equation with variable coefficients and plays a fundamental role in eigenvalue problems. The general form of sturm-Liouille equation

$$\frac{d}{dx}\left[p(x)\frac{dy}{dx}\right] + [\lambda w(x) - q(x)]y = 0. \tag{2.13}$$

Let's derive it from a classical PDE 1D heat equation or vibrating string equation

$$\frac{\partial^2 u}{\partial t^2} = c^2 \frac{\partial^2 u}{\partial x^2}. \tag{2.14}$$

Assume a solution by separation of variable method:

$$u(x,t) = X(x)T(t). \tag{2.15}$$

Substituting equation (2.15) in (2.14)

$$X(x)\frac{d^2T}{dt^2} = c^2 T(t)\frac{d^2X}{dx^2}. \tag{2.16}$$

Divide both sides by $X(x)T(t)$ of equation

(2.16)

$$\frac{1}{T}\frac{d^2T}{dt^2} = c^2\frac{1}{X}\frac{d^2X}{dx^2} = -\lambda. \tag{2.17}$$

The differential equations of time part and space part are

$$\frac{d^2T}{dt^2} + \lambda T = 0, \tag{2.18}$$

$$\frac{d^2X}{dx^2} + \frac{\lambda}{c^2}X = 0. \tag{2.19}$$

This spatial ODE is a simple Sturm–Liouville problem with $p(x) = 1, w(x) = 1, q(x) = 0$. Solutions $y_n(x)$ are orthogonal and useful for Fourier-type series expansions.

2.8 Superposition Principle

The superposition principle is a fundamental concept in linear partial differential equations (PDEs). It states that if two or more functions are solutions to a linear PDE, then any linear combination of these functions is also a solution to the same PDE [52].

Let's consider a linear PDE of the form,

$$L(u) = f, \tag{2.20}$$

where L is a place holder for any linear PDE operator (e.g., Laplacian, wave operator, heat operator), u is the unknown function, and f is a given function. If u_1 and u_2 are two solutions to the PDE, i.e.,

$$L(u_1) = f_1, \tag{2.21}$$

$$L(u_2) = f_2. \tag{2.22}$$

Then, the superposition principle states that any linear combination of u_1 and u_2 is also a solution to the PDE,

$$u = c_1u_1 + c_2u_2, \tag{2.23}$$

where c_1 and c_2 are arbitrary constants. To derive the superposition principle, we can use the linearity property of the differential operator L. Specifically, we can

write,

$$L(u) = L(c_1u_1 + c_2u_2). \tag{2.24}$$

If $f_1 = f_2 = f$, then we have,

$$L(u) = c_1f + c_2f = (c_1 + c_2)f. \tag{2.25}$$

This shows that the linear combination $u = c_1u_1 + c_2u_2$ is indeed a solution to the PDE.

2.9 Wave Equation

The wave equation is a fundamental partial differential equation that describes the propagation of waves in various physical systems [53]. Let's consider a small segment of the string between x and $x + \Delta x$.

The net force acting on the segment is,

$$F = T\sin(\theta(x + \Delta x)) - T\sin(\theta(x)). \tag{2.26}$$

Using the small-angle approximation,

$\sin(\theta) \approx \tan(\theta) = \frac{\partial y}{\partial x}$, we get:

$$F \approx T\frac{\partial y}{\partial x}(x + \Delta x) - T\frac{\partial y}{\partial x}(x). \tag{2.27}$$

After simplifying, the force will become:

$$F \approx T\frac{\partial^2 y}{\partial x^2}\Delta x. \tag{2.28}$$

The mass of the segment is $\mu\Delta x$, and its acceleration is $\frac{\partial^2 y}{\partial t^2}$. Applying Newton's second law, we get:

$$\mu\Delta x\frac{\partial^2 y}{\partial t^2} = T\frac{\partial^2 y}{\partial x^2}\Delta x. \tag{2.29}$$

Dividing both sides by Δx of equation (2.29)

$$\mu \frac{\partial^2 y}{\partial t^2} = T \frac{\partial^2 y}{\partial x^2}. \tag{2.30}$$

Rearranging the equation (2.30), we get:

$$\frac{\partial^2 y}{\partial t^2} = \frac{T}{\mu} \frac{\partial^2 y}{\partial x^2}. \tag{2.31}$$

This is the wave equation for a string, where $c = \sqrt{\frac{T}{\mu}}$ is the speed of the wave.

$$\frac{\partial^2 y}{\partial t^2} = c^2 \frac{\partial^2 y}{\partial x^2}. \tag{2.32}$$

The wave equation describes the propagation of waves in various physical systems, including strings, membranes, and electromagnetic fields.

2.10 Separation of Variable Method

The separation of variables method is a mathematical technique used to solve homogenous and linear types of partial differential equations (PDEs) by reducing them to simpler ordinary differential equations (ODEs). The central idea is to assume that the solution of a PDE can be written as a product of functions, where each function depends on only one of the independent variables. For example, in a problem involving both space and time variables, we assume a solution of the form $u(x,t) = X(x)T(t)$. Substituting this product into the original PDE allows the equation to be separated into two parts: one depending only on x and the other only on t.

Since these two sides are equal for all values of the variables, each must be equal to the same constant—often called the separation constant. This process transforms the original PDE into two ODEs, which are usually easier to solve. The solutions to these ODEs are then combined to form the general solution of the original PDE. This method is especially effective for linear and homogeneous equations with well-defined boundary and initial conditions, and it often leads to solutions

in the form of infinite series, such as Fourier series, representing different modes or harmonics of the system.

Chapter 3

Acoustic Attenuation from Single Wire Mesh

Wire mesh is a grid-like structure made by weaving or welding metal wires together, forming a pattern of interconnected openings. It is commonly made from materials such as steel, aluminum, copper, or stainless steel and comes in different sizes, thicknesses, and configurations. Wire mesh can attenuate acoustic waves through multiple mechanisms, including viscous losses, thermal effects, diffraction, and resonance.

The attenuation depends on parameters such as mesh size, wire thickness, porosity, material, and wave frequency. In this chapter, we examine acoustic wave propagation and scattering in a rectangular waveguide with a wire mesh. The governing boundary value problems (BVPs) include Helmholtz equations, rigid boundary condition and wire mesh conditions. The eigenfunctions in respective duct regions are orthogonal in nature. This chapter includes two problems.

- The first problem consists of the duct regions comprises compressible fluid with wire mesh in an infinite rectangular waveguide at $\hat{x} = 0$.
- The second problem is the wire mesh backed by a cavity in a semi infinite rectangular waveguide at $\hat{x} = d$.

3.1 Acoustic Attenuation Using Wire Mesh Backed by Cavity

Consider acoustic wave propagation in an infinite rectangular waveguide, having a wire mesh at $\hat{x} = 0$, as shown in Figure 3.1. This acoustic propagation in a waveguide having two regions $\hat{\Phi}_1$ and $\hat{\Phi}_2$, that are bounded by rigid walls at $\hat{y} = 0$ and 1. The insides of the regions $\hat{\Phi}_1$ and $\hat{\Phi}_2$ are filled with compressible fluid of density ρ_o having sound speed c_o. The geometry of the problem is shown in Figure 3.1.

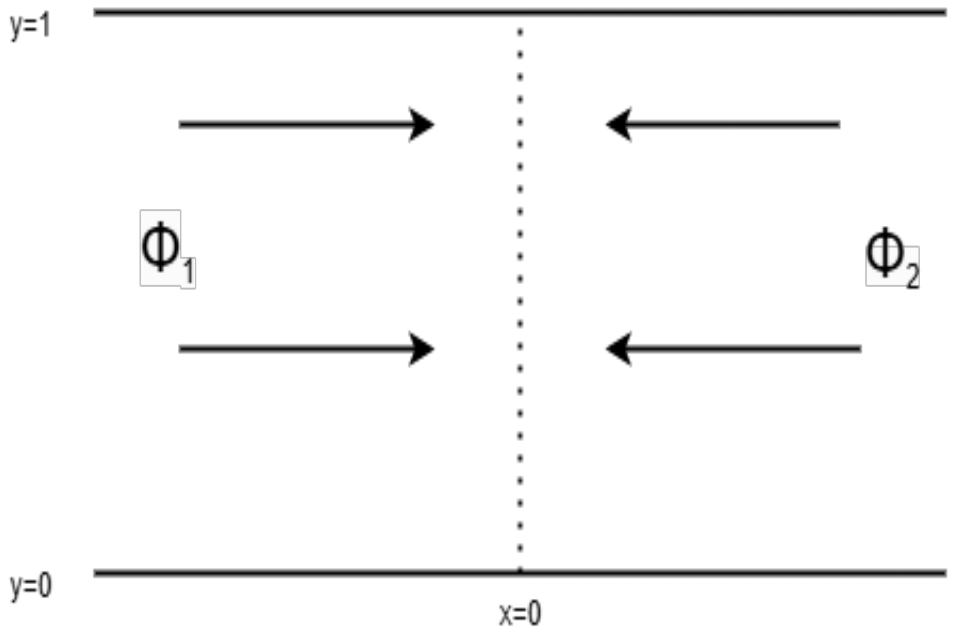

FIGURE 3.1: Infinite rectangular waveguide

We investigate a classical problem where acoustic waves propagate through a two-dimensional, horizontally oriented waveguide. The waveguide consists of two semi-infinite regions joined at a vertical interface and has a height of a units within a standard Cartesian coordinate system (see Figure 3.1).

The lower wall of the waveguide is positioned along the $\hat{y} = 0$ axis and extends infinitely in the $\hat{x}$-direction ($-\infty < \hat{x} > \infty$). The interior of the duct is filled with a compressible fluid, characterized by density ρ and sound speed c_0. It is important to note that the hat symbol indicates dimensional variables. The propagation of

acoustic waves within the fluid is described by the wave equation.

$$\frac{\partial^2\hat{\phi}}{\partial\hat{x}^2}+\frac{\partial^2\hat{\phi}}{\partial\hat{y}^2}=\frac{1}{c^2}\frac{\partial^2\hat{\phi}}{\partial\hat{t}^2}, \tag{3.1}$$

where $\hat{\Phi}$ is fluid potential and the acoustic pressure $\hat{p}$ and velocity $\hat{v}$ are related to the $\hat{\Phi}$ as $\hat{p}=\rho\frac{\partial\hat{\Phi}}{\partial t}$ and $\hat{v}=\nabla\hat{\Phi}$. The boundaries of the waveguide are a combination of rigid and impedance-type conditions. The mathematical form of these boundary conditions can be written from the definition of acoustic impedance ($\hat{Z}$) that is

$$\text{Impedance}=\frac{\text{pressure}}{\text{Normal velocity}},$$

$$\hat{Z}=\frac{\hat{p}}{\hat{n}.\hat{v}}, \tag{3.2}$$

where $\hat{n}$ is unit vector directed into the surface, for rigid condition, $\hat{Z}$ is undefined then (3.2) leads to

$$\hat{n}.\nabla\Phi=0. \tag{3.3}$$

Thus at $\hat{x}\leq 0$ for $\hat{y}=0$, we obtain the rigid condition from (3.3) as

$$\frac{\partial\hat{\phi}}{\partial\hat{y}}=0,\quad \hat{y}=0,1. \tag{3.4}$$

Now, for $\hat{x}\geq 0$,, impedance condition (3.2) for $\hat{y}=0$ leads to

$$\hat{Z}\frac{\partial\hat{\phi}}{\partial y}=-\rho\frac{\partial\hat{\phi}}{\partial t},\quad \hat{y}=0. \tag{3.5}$$

Likewise, for $\hat{y}=1$, we obtain the impedance condition from (3.3) as

$$\hat{Z}\frac{\partial\hat{\phi}}{\partial y}=-\rho\frac{\partial\hat{\phi}}{\partial t},\quad y=1. \tag{3.6}$$

Assuming the harmonic time dependence $e^{-i\omega\hat{t}}$, we can write

$$\left.\begin{aligned}\hat{\phi}(\hat{x},\hat{y},\hat{t})&=\hat{\Phi}(\hat{x},\hat{y})e^{-i\omega\hat{t}},\\ \hat{P}(\hat{x},\hat{y},\hat{t})&=\hat{p}(\hat{x},\hat{y})e^{-i\omega\hat{t}},\\ \hat{V}(\hat{x},\hat{y},\hat{t})&=\hat{v}(\hat{x},\hat{y})e^{-i\omega\hat{t}}.\end{aligned}\right\} \tag{3.7}$$

To make use of (3.7), we will transform (3.1) and (3.4)-(3.6) as:

$$\left\{\frac{\partial^2}{\partial\hat{x}^2}+\frac{\partial^2}{\partial\hat{y}^2}+\hat{k}^2\right\}\hat{\Phi}(\hat{x},\hat{y})=0, \tag{3.8}$$

$$\frac{\partial\hat{\Phi}}{\partial\hat{y}}=0, \quad \hat{y}=0,1, \tag{3.9}$$

$$\hat{Z}\frac{\partial\hat{\Phi}}{\partial y}=-i\omega\rho\hat{\Phi}, \quad y=0, \tag{3.10}$$

$$\hat{Z}\frac{\partial\hat{\Phi}}{\partial y}=i\omega\rho\hat{\Phi}, \quad y=1. \tag{3.11}$$

The above problem can be is non-dimensionalized by using the following transformation

$$\left.\begin{aligned}\hat{x}&=x,\\ \hat{y}&=y,\\ \omega\hat{t}&=t,\\ \hat{\Phi}&=\Phi.\end{aligned}\right\} \tag{3.12}$$

By using transformation (3.12), dimensionless form of is written as

$$\left\{\frac{\partial^2}{\partial x^2}+\frac{\partial^2}{\partial y^2}+k^2\right\}\Phi(x,y)=0. \tag{3.13}$$

The wave number k is normalized as $k=\hat{k}a$, and the fluid velocity potential is represented by the dimensionless function $\Phi(x,y)$, which has the following form:

$$\Phi(x,y)=\begin{cases}\Phi_1(x,y), & 0\le y\le 1, x<0,\\ \Phi_2(x,y), & 0\le y\le 1, x>0.\end{cases}$$

The fluid potentials in duct are represented by Φ_1 and Φ_2, respectively. As the fluid potential $\Phi_1(x,y)$ satisfy the Helmholtz's equations from written as

$$\frac{\partial^2\Phi_1}{\partial x^2}+\frac{\partial^2\Phi_1}{\partial y^2}+k^2\Phi_1=0, \tag{3.14}$$

where $\Phi_1(x, y)$ is a field potential and $k = \frac{w}{c}$ is known as wave number. The boundary conditions for region Φ_1 and Φ_2 are

$$\frac{\partial \Phi_1}{\partial y} = 0, \quad y = 0, \tag{3.15}$$

$$\frac{\partial \Phi_1}{\partial y} = 0, \quad y = 1. \tag{3.16}$$

The boundary value problem defined in (3.14)-(3.16) can be solved by using the separation of variable method. By separation of variable method we assume that

$$\Phi_1 = X(x)Y(y). \tag{3.17}$$

Employing (3.17) into (3.14) we fetch the following equation

$$\frac{Y''}{Y} = \frac{X''}{X} + k^2 = -\lambda_n^2. \tag{3.18}$$

Ordinary differential equation for $(Y(y))$ from (3.18), can be written as

$$\frac{Y''}{Y} + \lambda_n^2 = 0. \tag{3.19}$$

From (3.19), the solution of the ordinary differential equation for $Y(y)$ of region Φ_1 is

$$Y = c_1 \cos(\lambda_n y) + c_2 \sin(\lambda_n y), \tag{3.20}$$

where c_1 and c_2 are the arbitrary constants, which can be found with the help of boundary conditions. By differentiating equation (3.20), we obtain

$$Y' = -c_1 \sin(\lambda_n y) + c_2 \cos(\lambda_n y). \tag{3.21}$$

Employing the boundary condition of (3.15) into (3.21), we get

$$c_2 = 0. \tag{3.22}$$

By substituting (3.22) into (3.20) , we attain

$$Y = c_1 \cos(\lambda_n y). \tag{3.23}$$

Now by invoking (3.23), for nontrivial solutions of (3.16), reveals $\sin(\lambda_n y) = 0$, which gives $\lambda_n = n\pi$ and $n = 1, 2, 3, \ldots$ which gives the eigenfunctions

$$Y = Y_n = \cos(\lambda_n y) = \cos(n\pi y). \tag{3.24}$$

The differential equation for $X(x)$ from (3.18), we obtain

$$\frac{X''}{X} + k^2 + \lambda_n^2 = 0. \tag{3.25}$$

From (3.25), the solution of ordinary differential equation for $X(x)$ is

$$X = c_3 e^{-i\eta_n x}, \tag{3.26}$$

where $\eta_n = \sqrt{k^2 + \lambda_n^2}$ and c_3 is an arbitrary constant. Now substituting (3.24) and (3.26) into (3.17), we get the solution of Φ_1 and then applying the superposition principle we attain the following solution,

$$\Phi_1 = \sum_{n=o}^{\infty} A_n \Phi_n e^{-i\eta_n x} + \sum_{n=0}^{\infty} a_n(x) \Phi_n. \tag{3.27}$$

The region Φ_2 also satisfy the Helmholtz's equations, which have same field potential (x, y) and the boundary conditions are

$$\frac{\partial^2 \Phi_2}{\partial x^2} + \frac{\partial^2 \Phi_2}{\partial y^2} + k^2 \Phi_2 = 0, \tag{3.28}$$

$$\frac{\partial \Phi_2}{\partial y} = 0, \quad y = 0, \tag{3.29}$$

$$\frac{\partial \Phi_2}{\partial y} = 0, \quad y = 1. \tag{3.30}$$

To solve the above mentioned equation of system ((3.28)-(3.30)) we apply the separation of variable method. For the separation of variable method we assume that,

$$\Phi_2 = X(x)Y(y). \tag{3.31}$$

Substituting (3.31) into (3.28) after we obtain the following solution, which is in the form of differential equation of $X(x)$ and $Y(y)$

$$\frac{Y''}{Y} = \frac{X''}{X} + k^2 = -\tau^2. \tag{3.32}$$

The ordinary differential equation of $Y(y)$ from (3.32) is

$$\frac{Y''}{Y} + \tau^2 = 0. \tag{3.33}$$

To solve the differential equation of $Y(y)$ (3.33), we get

$$Y = c_3 \cos(\tau_n y) + c_4 \sin(\tau_n y). \tag{3.34}$$

To satisfy the given boundary condition, differentiate (3.19) with respect to y

$$Y' = -c_3 \sin(\tau_n y) + c_4 \cos(\tau_n y), \tag{3.35}$$

where c_3 and c_4 are the arbitrary constants. The values of c_3 and c_4 can be found by using (3.29) and (3.30) into (3.35), which gives the value of $c_3 = 0$ and the eigenvalues for τ_n are $\tau_n = n\pi$, where $n = 1, 2, 3, \ldots$ and eigenfunctions are

$$Y = Y_n = \cos(n\pi y). \tag{3.36}$$

Now from (3.32) the differential equation for $X(y)$ is

$$\frac{X''}{X} + k^2 + \tau^2 = 0. \tag{3.37}$$

To solve the differential equation of (3.37) we get the following solution of Φ_2

$$X = c_5 e^{i\eta_n x}, \tag{3.38}$$

where $\eta_n = \sqrt{k^2 + \tau_n^2}$ and c_5 is the arbitrary constant. Now applying the superposition principle on (3.36) and (3.38) which gives the solution for region Φ_2 as

$$\Phi_2 = \sum_{n=0}^{\infty} B_n \Phi_n e^{i\eta_n x}. \tag{3.39}$$

3.2 Wire Mesh in Infinite Waveguide

This problem involves a wire mesh placed inside a two-dimensional rectangular waveguide. The waveguide extends infinitely in the x-direction ($-\infty \leq x \leq \infty$) and spans from $y = 0$ to $y = 1$ in the vertical direction. A wire mesh is located at $x = 0$, acting as an interface within the waveguide. To solve the system of mathematical equations governing wave propagation in this setup, appropriate boundary conditions are applied at the location of the wire mesh ($x = 0$).

These boundary conditions—referred to as wire boundary conditions which are essential for determining the unknown constants A_n and B_n, which appear in the solutions for the wave fields in the regions on either side of the mesh (commonly denoted as Φ_1 and Φ_2). In acoustic waveguide problems, the presence of a discontinuity, such as a wire mesh requires special treatment at the interface. The wire boundary condition enforces physical continuity rules, like pressure and velocity matching across the mesh. Solving the system with this condition allows us to find the amplitudes (constants A_n and B_n) that describe how the wave behaves in each region, in fully characterizing the wave interaction with the mesh. The reflection and transmission of acoustic waves in a rectangular waveguide with wire-mesh interfaces are described by the wave fields Φ_1 and Φ_2 are

$$\Phi_1 = \sum_{n=0}^{\infty} A_n \Phi_n e^{-i\eta_n x} + \sum_{n=0}^{\infty} a_n(x) \Phi_n \tag{3.40}$$

$$\Phi_2 = \sum_{n=0}^{\infty} B_n \Phi_n e^{i\eta_n x}, \tag{3.41}$$

where

$$a_n(x) = \delta_{n0} e^{i\eta_n x}. \tag{3.42}$$

The boundary conditions of wire mesh in an infinite rectangular waveguide are

$$\frac{\partial \Phi_1}{\partial x} = \frac{\partial \Phi_2}{\partial x}, \quad x = 0, \tag{3.43}$$

$$\Phi_2 - \Phi_1 = \frac{iz}{k}\frac{\partial \Phi_2}{\partial x}, \quad x = 0, \tag{3.44}$$

where z is the impedance normalized by $\rho_o c_o$. The resistance z is a positive real number (remarkably independent of the frequency as long as the wavelength is much larger than the mesh thickness), that characterizes the lossy effect of the wiremesh and which "microscopically" originates from the viscous friction of the oscillatory acoustic creeping flow in the pores. Since the positive impedance z is induced by the viscous oscillatory flow in the pores of the wiremesh, z increases when the density of wires increases, implying a decrease in the size of the pores. Now by using the wire mesh boundary condition of (3.43) into (3.40) and (3.41) into we get

$$i\eta_n \sum_{n=0}^{\infty} \delta_{n0}\Phi_n - i\eta_n \sum_{n=0}^{\infty} A_n \Phi_n = i\eta_n \sum_{n=0}^{\infty} B_n \Phi_n. \tag{3.45}$$

Orthogonality relation allows to decompose the complex fields (like pressure, velocity, or displacement) into a sum of modes (e.g., sine or cosine functions), where each mode can be treated independently. So for applying the orthogonality relation, multiplying the equation (3.45) by Φ_m and integrating with respect to y from 0 to 1, we obtain

$$\sum_{n=0}^{\infty} \delta_{n0} \int_0^1 \Phi_m \Phi_n dy - \sum_{n=0}^{\infty} A_n \int_0^1 \Phi_m \Phi_n dy = \sum_{n=0}^{\infty} B_n \int_0^1 \Phi_m \Phi_n dy. \tag{3.46}$$

Employing the orthogonality relation in equation (3.46) and after simplifying we gain

$$B_n = \delta_{n0} - A_n. \tag{3.47}$$

Now we applying the boundary condition, for this using (3.40) and (3.41) into (3.44), we obtain

$$\sum_{n=0}^{\infty} B_n \Phi_n - \sum_{n=0}^{\infty} A_n \Phi_n - \sum_{n=0}^{\infty} \delta_{n0}\Phi_n = \frac{iz}{k} i\eta_n \sum_{n=0}^{\infty} B_n \Phi_n. \tag{3.48}$$

The eigenfunction orthogonal in nature in Φ_1 and Φ_2, so for the orthogonality relation we multiplying equation (3.48) with Φ_m and integrating with respect to Y from 0 to 1

$$\sum_{n=0}^{\infty} B_n \int_0^1 \Phi_m \Phi_n dy - \sum_{n=0}^{\infty} A_n \int_0^1 \Phi_m \Phi_n dy - \sum_{n=0}^{\infty} \delta_{n0} \int_0^1 \Phi_m \Phi_n dy = -\frac{\eta_n z}{k} \sum_{n=0}^{\infty} B_n \int_0^1 \Phi_m \Phi_n dy. \tag{3.49}$$

Now by using the orthogonality relation in equation (3.49) and after simplifying we get

$$B_n - \delta_{n0} - A_n = -\frac{\eta_n z}{k} B_n. \tag{3.50}$$

From equation (3.47) into (3.50) and after simplifications we obtain the value of A_n as

$$A_n = \frac{\eta_n z \delta_{n0}}{2k + \eta_n z}. \tag{3.51}$$

By putting the value of A_n (3.51) into (3.47) equation we obtain the value of B_n is

$$B_n = \frac{2k\delta_{n0}}{2k + \eta_n z}. \tag{3.52}$$

3.3 Wire Mesh Backed by Cavity

In this configuration Figure 3.2, a wire mesh is placed at $x = 0$ within a two-dimensional rectangular waveguide that extends infinitely in the x-direction and spans from $y = 0$ to $y = 1$ in height. The region $x > 0$ is a cavity that terminates at a rigid wall located at $x = d$. The wire mesh acts as a partially transmitting and reflecting interface for the acoustic wave, while the rigid boundary at $x = d$ reflects all incoming wave energy due to its zero normal velocity condition. This setup creates a resonant cavity between the wire mesh and the rigid wall, where acoustic waves reflect and interfere, depending on the cavity length and the frequency of the incident wave.

The presence of the wire mesh modifies the wave transmission and reflection characteristics at $x = 0$, depending on its mechanical properties (such as tension and

impedance). The rigid boundary condition at $x = d$ mathematically imposes a Neumann condition, zero normal derivative of pressure ensuring no particle motion into the wall. This model is crucial for understanding wave interactions in layered or structured acoustic systems and is commonly used in designing noise control devices and acoustic filters. In this problem, an acoustic wave propagates through a semi-infinite rectangular waveguide with a rigid boundary condition imposed at $x = d$. The geometry of the acoustic wave in semi infinite rectangular wave guide shown in Figure 3.2.

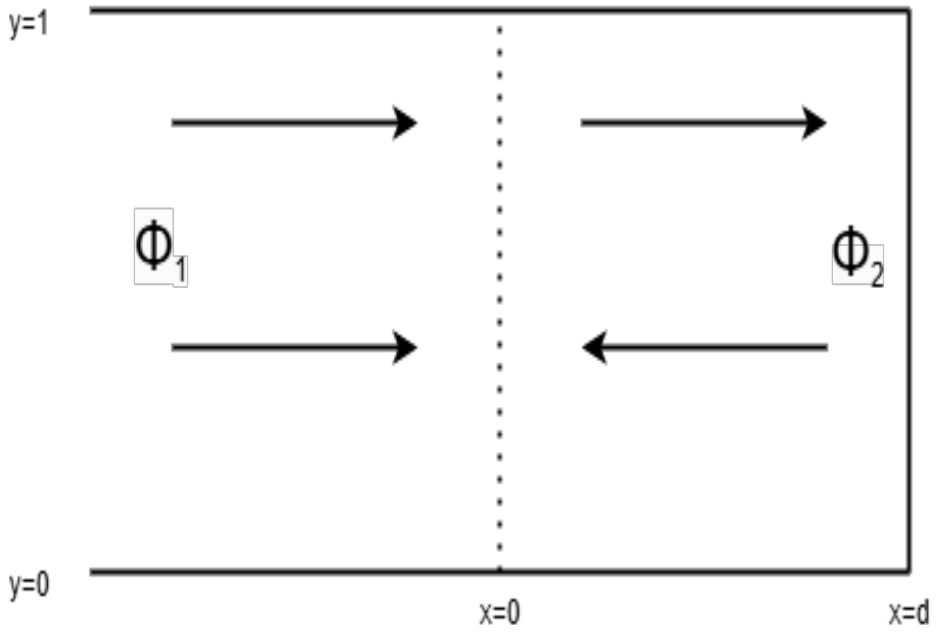

FIGURE 3.2: semi infinite rectangular wave guide

Here the acoustic wave equation for semi infinite rectangular waveguide with wire-mesh backed by cavity at $x = 0$, for region Φ_1 and Φ_2 are

$$\Phi_1 = \sum_{n=0}^{\infty} A_n \Phi_n e^{-i\eta_n x} + \sum_{n=0}^{\infty} \delta_{n0} e^{i\eta_n x} \Phi_n, \tag{3.53}$$

$$\Phi_2 = \sum_{n=0}^{\infty} B_n \Phi_n e^{i\eta_n x} + \sum_{n=0}^{\infty} C_n \Phi_n e^{-i\eta_n x}. \tag{3.54}$$

The rigid boundary condition at $x = d$, and wire mesh conditions at $x = 0$ are

$$\frac{\partial \Phi_1}{\partial x} = \frac{\partial \Phi_2}{\partial x}, \quad x = 0, \tag{3.55}$$

$$\Phi_2 - \Phi_1 = \frac{iz}{k}\frac{\partial \Phi_2}{\partial x}, \quad x = 0, \tag{3.56}$$

$$\frac{\partial \Phi_2}{\partial x} = 0, \quad x = d. \tag{3.57}$$

Now utilizing (3.53) and (3.54) into (3.57), and after modification we obtain

$$\sum_{n=0}^{\infty} B_n \Phi_n e^{i\eta_n d} = \sum_{n=0}^{\infty} C_n \Phi_n e^{-i\eta_n d}. \tag{3.58}$$

For applying orthogonality relation, multiplying equation (3.58) with Φ_m and integrating with respect to y from 0 to 1, we get

$$\sum_{n=0}^{\infty} B_n e^{i\eta_n d} \int_0^1 \Phi_m \Phi_n dy = \sum_{n=0}^{\infty} C_n e^{-i\eta_n d} \int_0^1 \Phi_m \Phi_n dy. \tag{3.59}$$

Employing the orthogonality relation in equation (3.59) and after modification we get

$$C_n = B_n e^{2i\eta_n d}. \tag{3.60}$$

By using equation (3.53) and (3.54) into (3.55)

$$\sum_{n=0}^{\infty} \delta_{n0} \Phi_n - \sum_{n=0}^{\infty} A_n \Phi_n = \sum_{n=0}^{\infty} B_n \Phi_n - \sum_{n=0}^{\infty} C_n \Phi_n. \tag{3.61}$$

Multiplying equation (3.61) with Φ_m and integrating with respect to y from 0 to 1 to obtain

$$\sum_{n=0}^{\infty} \delta_{n0} \int_0^1 \Phi_m \Phi_n dy - \sum_{n=0}^{\infty} A_n \int_0^1 \Phi_m \Phi_n dy = \sum_{n=0}^{\infty} B_n \int_0^1 \Phi_m \Phi_n dy \sum_{n=0}^{\infty} C_n \int_0^1 \Phi_m \Phi_n dy. \tag{3.62}$$

Using orthogonality relation in equation (3.62) and after simplifying we get

$$A_n = \delta_{n0} - B_n + C_n. \tag{3.63}$$

By Using equation (3.53) and (3.54) into (3.56)

$$\sum_{n=0}^{\infty} B_n \Phi_n + \sum_{n=0}^{\infty} C_n \Phi_n - \sum_{n=0}^{\infty} A_n \Phi_n + \sum_{n=0}^{\infty} \delta_{n0} \Phi_n = -\frac{\eta_n z}{k} [\sum_{n=0}^{\infty} B_n \Phi_n - \sum_{n=0}^{\infty} C_n \Phi_n]. \tag{3.64}$$

Multiplying equation (3.64) with Φ_m and integrating from 0 to 1, we get

$$\sum_{n=0}^{\infty} B_n \int_0^1 \Phi_m \Phi_n dy + \sum_{n=0}^{\infty} C_n \int_0^1 \Phi_m \Phi_n dy - \sum_{n=0}^{\infty} A_n \int_0^1 \Phi_m \Phi_n dy + \sum_{n=0}^{\infty} \delta_{n0} \int_0^1 \Phi_m \Phi_n dy = -\frac{\eta_n z}{k} [\sum_{n=0}^{\infty} B_n \int_0^1 \Phi_m \Phi_n dy - \sum_{n=0}^{\infty} C_n \int_0^1 \Phi_m \Phi_n dy]. \tag{3.65}$$

Using orthogonality relation in equation (3.65) and after simplification we get

$$B_n + C_n - \delta_{n0} - A_n = -\frac{\eta_n z}{k}(B_n - C_n). \tag{3.66}$$

Utilizing equation (3.63) into (3.66) and after rearranging, we obtain

$$C_n = 2B_n + \frac{z\eta_n}{k} B_n - \delta_{n0} - \frac{i\eta_n \delta_{n0}}{i\eta_n}. \tag{3.67}$$

Using equation (3.60) into (3.67)

$$B_n = \frac{2k\delta_{n0}}{2k + \eta_n z(1 - e^{2i\eta_n d})}. \tag{3.68}$$

Putting the value of B_n (3.50) into (3.60), we obtain

$$C_n = \frac{2k\delta_{n0} e^{2i\eta_n d}}{2k + \eta_n z(1 - e^{2i\eta_n d})}. \tag{3.69}$$

Utilizing the value of C_n (3.69) and B_n (3.68) into (3.63), we obtain the value of

$$A_n = \frac{\delta_{n0}(2ke^{2i\eta_n d} - \eta_n z(3 - e^{2i\eta_n d}))}{2k + \eta_n z(1 - e^{2i\eta_n d})}. \tag{3.70}$$

3.4 Numerical Results

This section provides a numerical solution to the problem discussed in the chapter, with the system truncated to N terms. The numerical computations are conducted using the PYTHON software, with the relevant parameters set to fixed values as: wire mesh dimensions impedance $z = 0$ kg/(m^{2}s) to $z = 1$ kg/m^2, speed of sound in air $c = 343.5$ m/s, wire mesh mass density of air $\rho = 1.3$ kg/m^3, frequency $f = 100$ Hz, density of wire mesh $\rho_m = 0.17$ kg/m^3 and spring constant $k = 1.82$. The number of terms considered is set to 10 to 70.

In Figure 3.3 The real parts of the velocities are plotted against the $y - axis$ at fixed $x = 0$ to $x = 0.1$. The two velocity components coincide, confirming the accuracy of the truncated solution at the specified frequency. In Figure 3.4 the real parts of velocities are shown against $y - axis$ at $f = 1000$ Hz. As the frequency increases, more modes are excited, yet the velocity components continue to coincide, validating the accuracy of the truncated solution at $f = 1000$ Hz. The Figure 3.5 displays the real parts of the velocities plotted along the $y - axis$ at $N = 70$ and $f = 1000$ Hz. As the frequency increases, the number of propagating modes also rises. The coincidence of both velocity components confirms the validity of the truncated solution at the specified frequency.

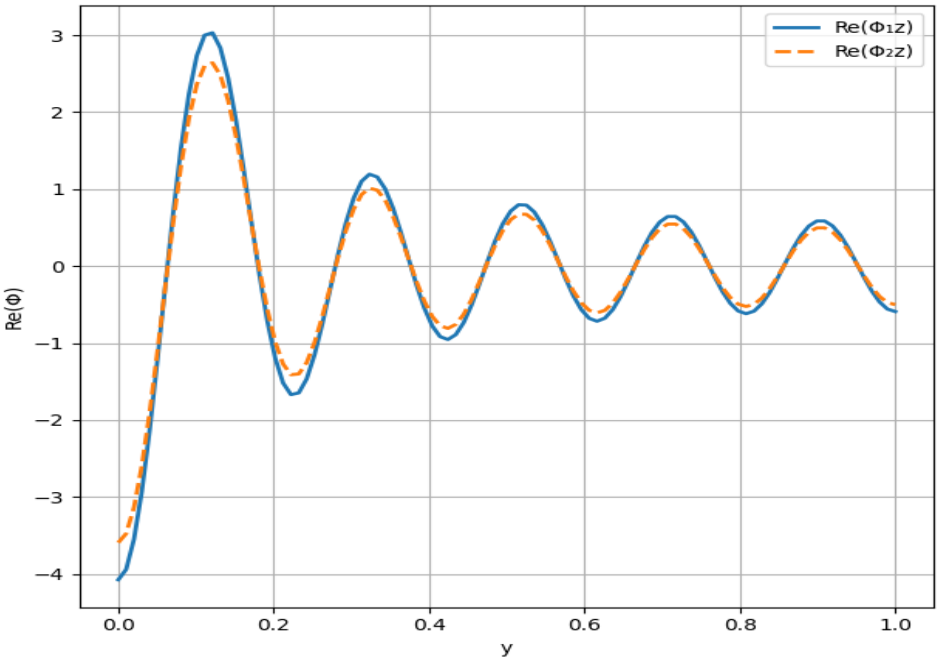

FIGURE 3.3: Real parts of the velocities against y-axis at $f = 100$ Hz

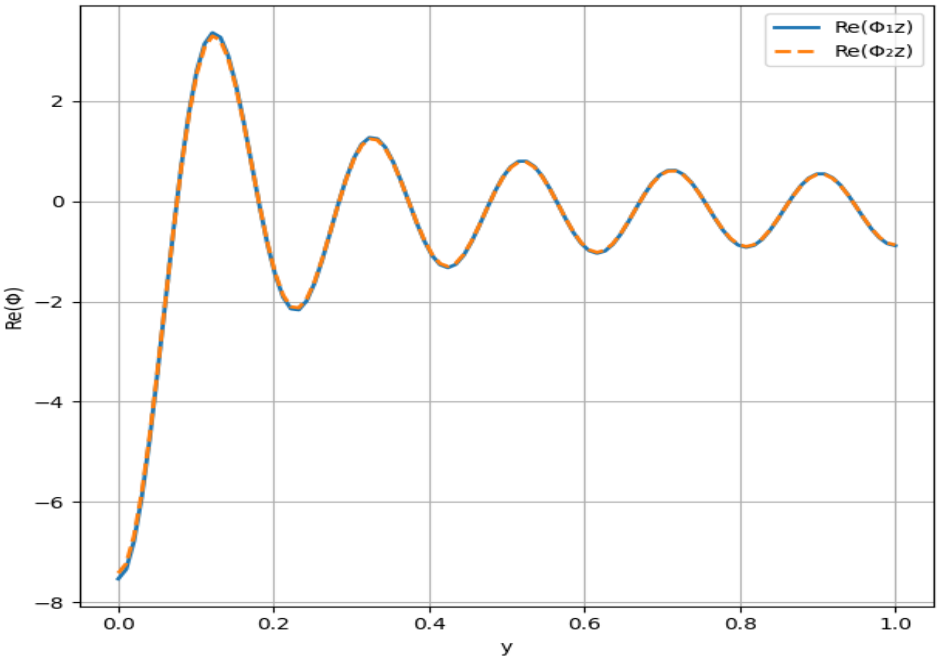

FIGURE 3.4: Real parts of the velocities against y-axis at $f = 1000$ Hz

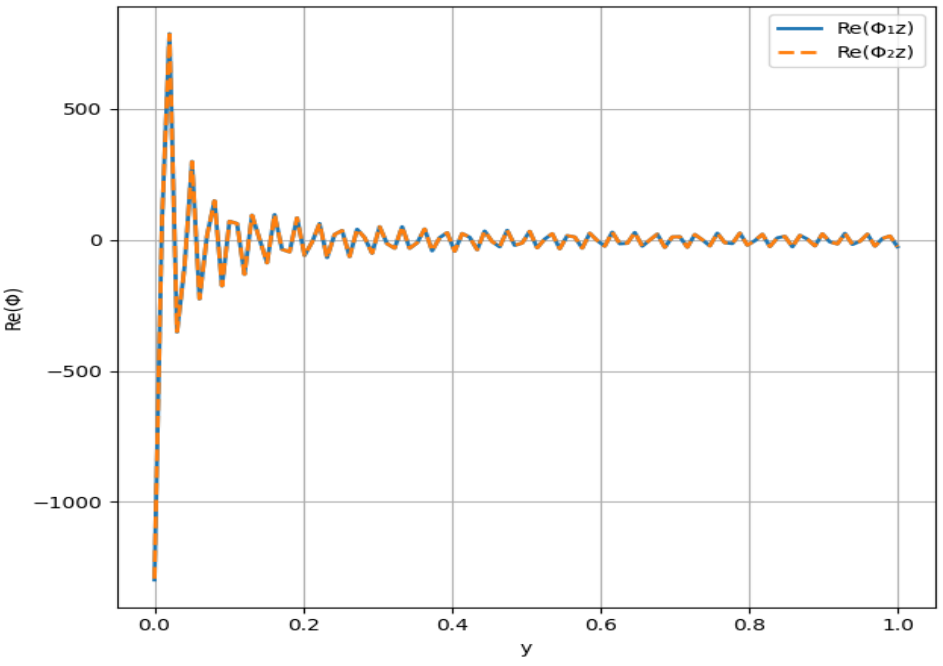

FIGURE 3.5: Real parts of the velocities against y-axis at $f = 2500$ Hz

The imaginary parts of the velocities are analyzed at different frequencies to further verify the accuracy of the truncated solution. Figure 3.6 at frequencies $f = 100$ Hz and $f = 1000$ Hz with $N = 10$ to $N = 70$, respectively. At each frequency, the velocity components are found to coincide, indicating that the truncated solution effectively captures the system's dynamics. Furthermore, the results show

that higher frequencies excite additional modes, as indicated by the increasing number of propagating modes observed in the velocity profiles Figure (3.3-3.7). As frequency increases, more wave modes become active or "propagate" through the system. These additional modes influence how energy is distributed and how the wave behaves within the waveguide. Ignoring them could lead to inaccurate predictions. Therefore, it's crucial to consider how frequency affects the number and behavior of these modes to fully understand and model the response of the system.

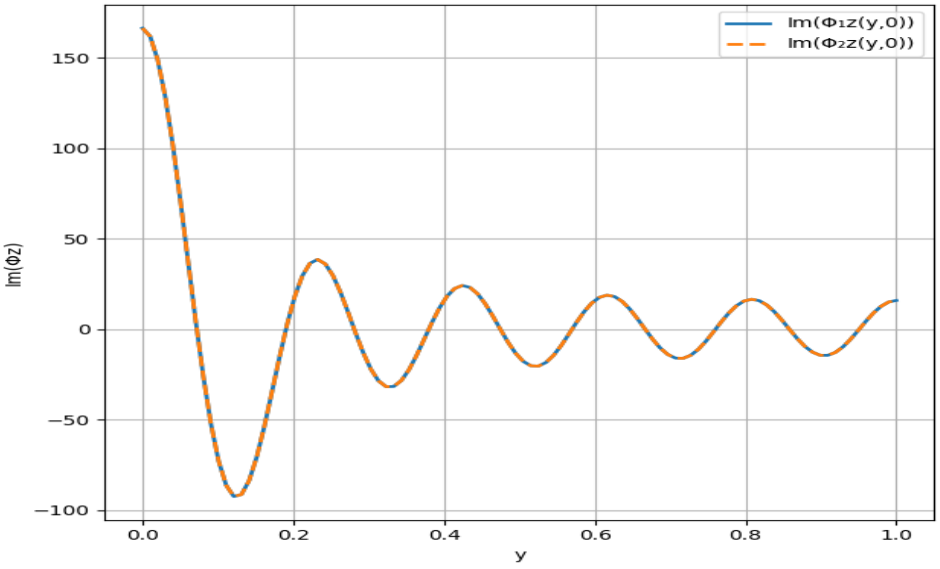

FIGURE 3.6: Real parts of the velocities against y-axis at $f = 100$ Hz

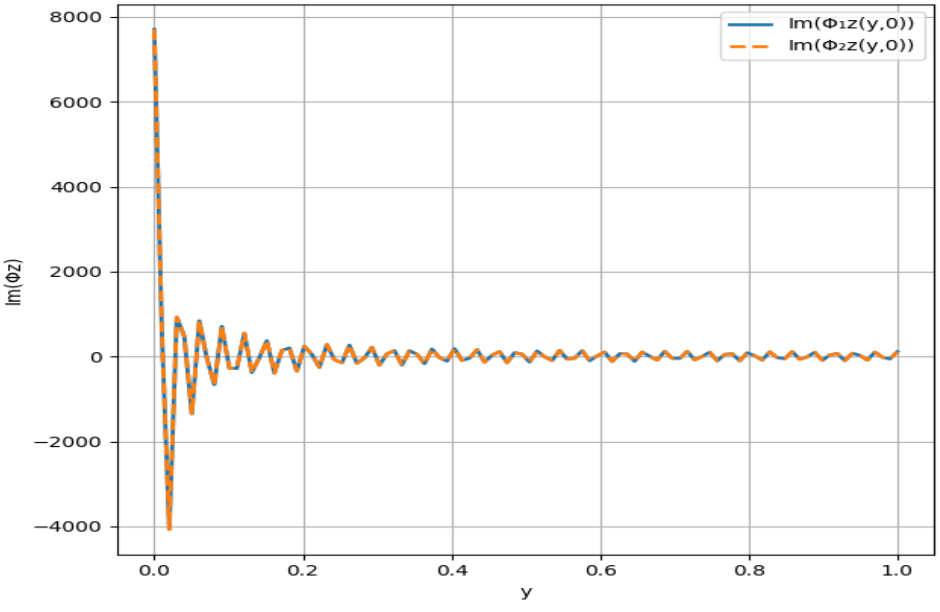

FIGURE 3.7: Real parts of the velocities against y-axis at $f = 1000$ Hz

The Figure (3.8-3.13) displays the real and imaginary parts of the pressure plotted along the y axis at a fixed position $x = 0$, for three different frequencies: $f = 100$ Hz, $f = 1000$ Hz, $f = 2500$ Hz. At each frequency, the real and imaginary pressure components closely overlap, confirming the accuracy of the truncated solution. Moreover, as the frequency increases, additional pressure modes are excited, as indicated by the increasingly complex structure in the pressure profiles. This behavior demonstrates that the number of propagating modes grows with frequency, highlighting the importance of accounting for higher modes in the analysis at elevated frequencies. In Figure 3.14, the relationship between frequency and the amplitude at A_0 is illustrated.

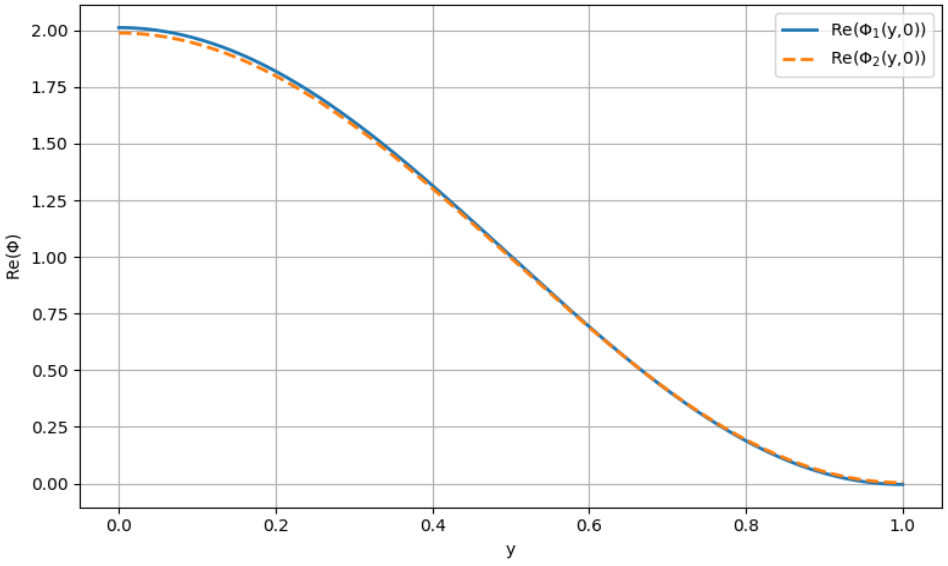

FIGURE 3.8: Real parts of pressures against y-axis at $f = 100$ Hz

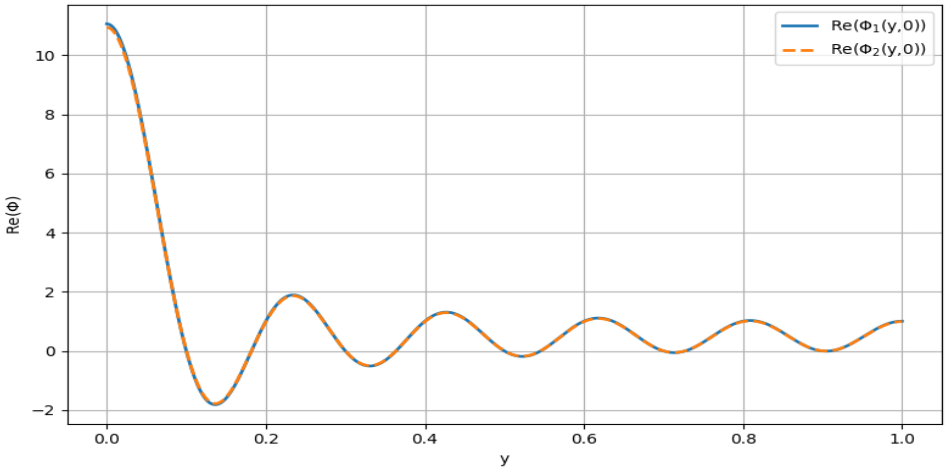

FIGURE 3.9: Real parts of pressures against y-axis at $f = 1000$ Hz

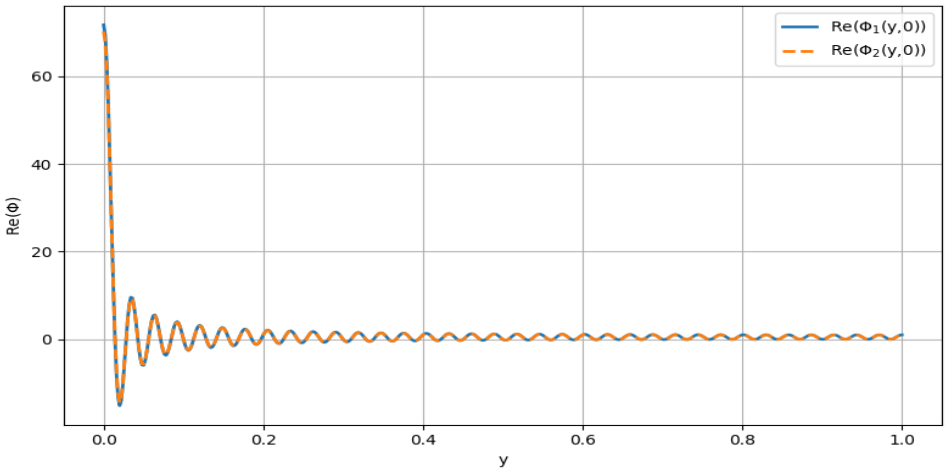

FIGURE 3.10: Real parts of pressures against y-axis at $f = 2500$ Hz

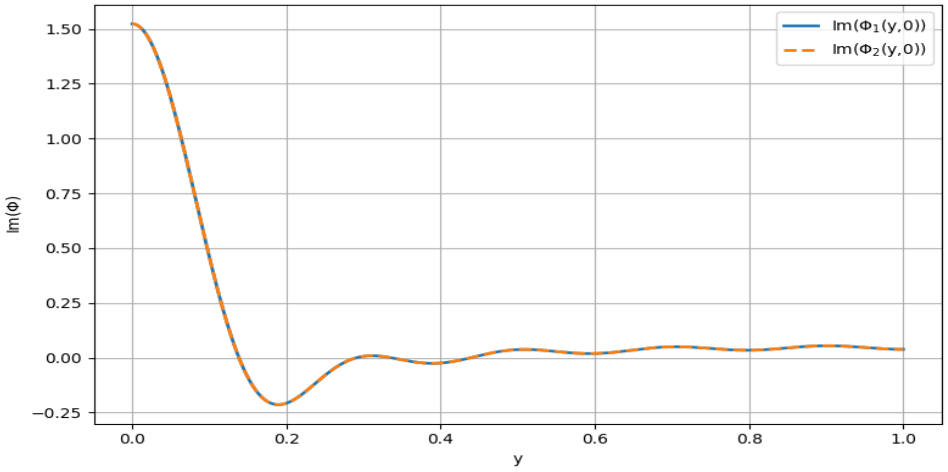

FIGURE 3.11: Imaginary parts of pressures against y-axis at $f = 100$ Hz

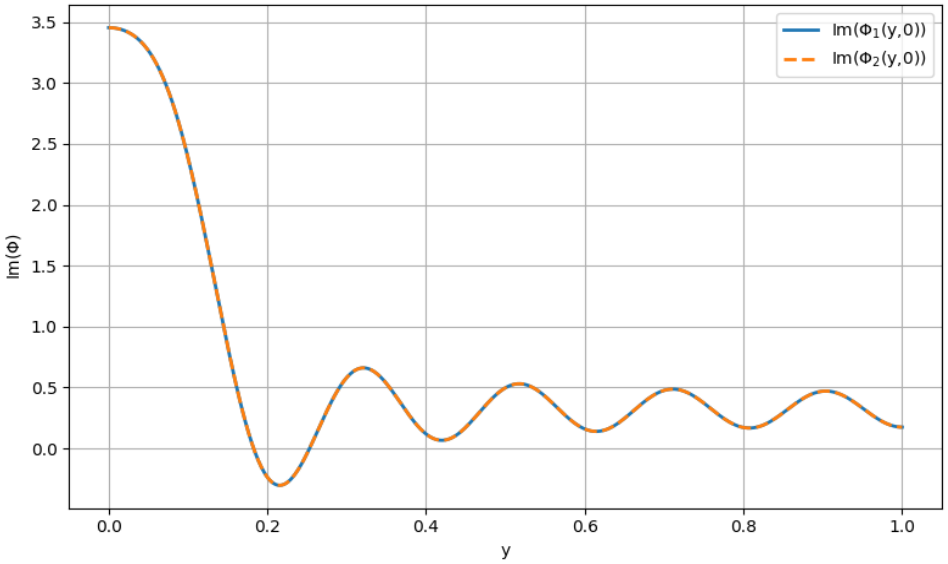

FIGURE 3.12: Imaginary parts of pressures against y-axis at $f = 1000$ Hz

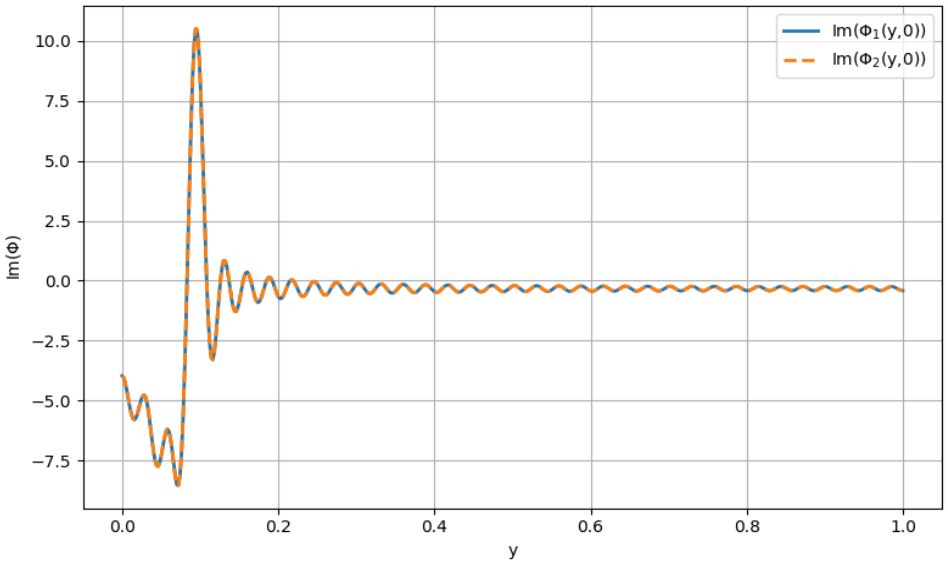

FIGURE 3.13: Imaginary parts of pressures against y-axis at $f = 2500$ Hz

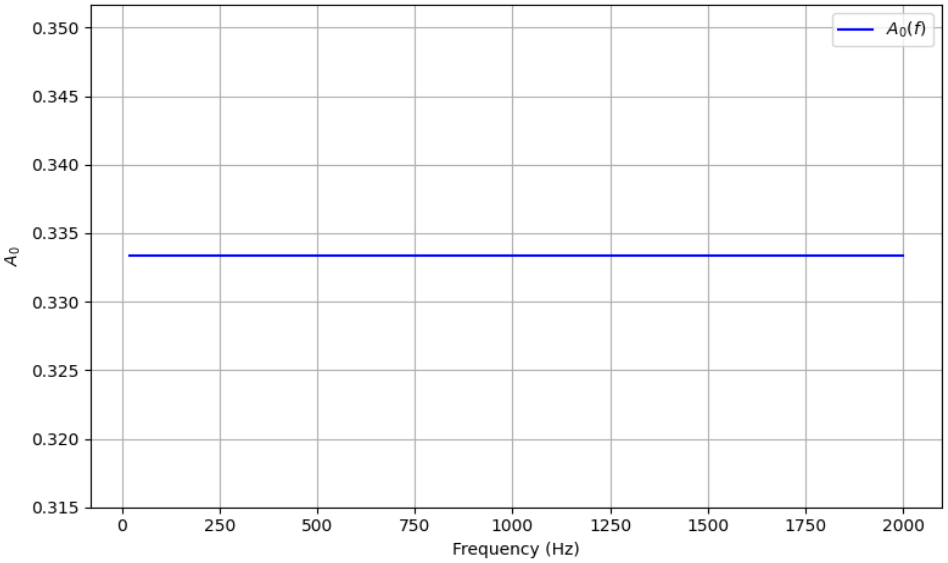

FIGURE 3.14: Frequency f against amplitude A_0

Chapter 4

Acoustic Attenuation from Two Wire Mesh

4.1 Introduction

This chapter explores the propagation and scattering of acoustic waves with wire-mesh at interfaces comprising rigid and soft boundaries. We are assuming an infinite rectangular waveguide that have two wire meshes at $x = -L$ and $x = L$. There are three regions of compressible fluid potentials Φ_1, Φ_2 and Φ_3, respectively. In this chapter, to solve this problem, we break down the configuration into two sub-problems. The first sub-problem is the symmetric problem, and the second sub-problem is the antisymmetric problem. This decomposition allows for separate analysis of each case, which can later be combined to form the complete solution.

4.2 Problem Formulation

The problem analyzed in this section involves a waveguide containing two wire-mesh interfaces positioned at $x = L$ and $x = -L$. The boundaries of the waveguide are rigid along the horizontal edges at $y = 0$ and $y = 1$, and the interior is filled with a compressible fluid that supports wave propagation. These wire meshes act

as semi-permeable interfaces that influence how acoustic waves are transmitted and reflected within the waveguide. The rigid boundaries at $y = 0$ and $y = 1$ imply that the wave cannot move the boundary vertically, enforcing zero normal velocity, a typical condition in acoustic waveguides with hard walls. The waveguide is filled with a compressible fluid (such as air), allowing acoustic waves to propagate. This setup is often used to study wave scattering, mode coupling, and resonance phenomena in ducts or layered acoustic structures. The geometrical configuration is shown in Figure 4.1.

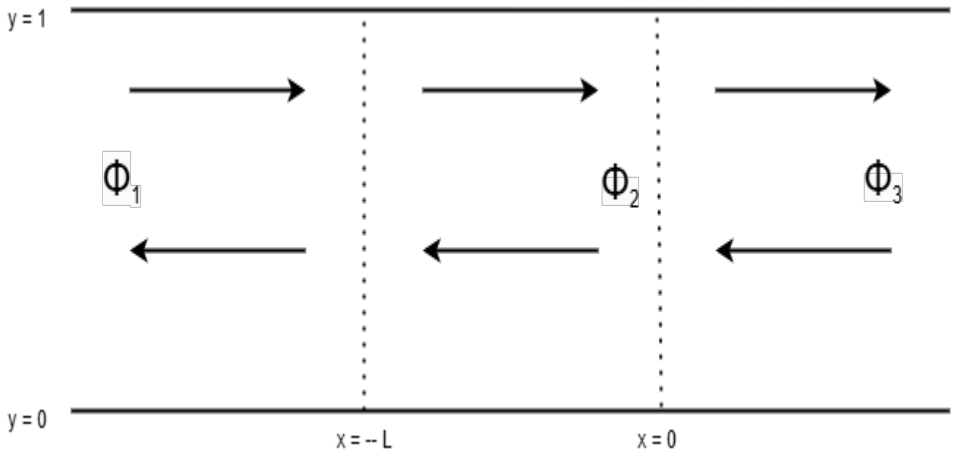

FIGURE 4.1: Infinite rectangular wave guide with two wire mesh

The governing boundary value problem consists of Helmholtz equations subject to both rigid wall and wire-mesh boundary conditions. To make the problem more manageable and to focus on fundamental behaviors rather than units, the equations and parameters are converted into dimensionless form. This process, called nondimensionalization, often involves scaling length, frequency, pressure, and other quantities by characteristic values. It allows for clearer identification of key parameters that control the system's response and makes the results applicable to a wider range of physical situations. The Helmholtz equations for region Φ_1, Φ_2, and Φ_3 the are

$$\frac{\partial^2 \Phi_1}{\partial x^2} + \frac{\partial^2 \Phi_1}{\partial y^2} + k^2 \Phi_1 = 0, \tag{4.1}$$

$$\frac{\partial^2 \Phi_2}{\partial x^2} + \frac{\partial^2 \Phi_2}{\partial y^2} + k^2 \Phi_2 = 0, \tag{4.2}$$

$$\frac{\partial^2 \Phi_3}{\partial x^2} + \frac{\partial^2 \Phi_3}{\partial y^2} + k^2 \Phi_3 = 0. \tag{4.3}$$

The boundary conditions for region Φ_1, Φ_2 and Φ_3 are,

$$\frac{\partial \Phi}{\partial y} = 0, \quad y = 0, \tag{4.4}$$

$$\frac{\partial \Phi}{\partial y} = 0, \quad y = 1. \tag{4.5}$$

Here $\Phi = \Phi_1, \Phi_2, \Phi_3$ and the boundary value problem defined in (4.1)-(4.5) can be solved by using the separation of variables method. By applying the separation of variable method for (4.1), (4.2) and (4.3) we assume that,

$$\Phi_n = X(x)Y(y). \tag{4.6}$$

Using (4.6) into (4.1), (4.2) and (4.3) we obtain

$$\frac{Y''}{Y} = \frac{X''}{X} + k^2 = -\alpha_n^2. \tag{4.7}$$

From (4.7) the solutions of ordinary differential equation for regions Φ_1, Φ_2 and Φ_3 are,

$$Y = C_5 \cos(\alpha_n y) + C_6 \sin(\alpha_n y). \tag{4.8}$$

where C_5 and C_6 are the arbitrary constants which can be found with the help of boundary conditions. After differentiating (4.8), we get

$$Y' = -C_5 \sin(\alpha_n y) + C_6 \cos(\alpha_n y). \tag{4.9}$$

At $y = 0$ the boundary condition (4.4) into (4.8) gives

$$C_6 = 0. \tag{4.10}$$

Now, putting the value of C_6 in (4.9) gives the following equation

$$Y' = -C_5 \sin(\alpha_n y). \tag{4.11}$$

The boundary condition (4.5) into (4.11) leads to the following eigen values, $\sin(\alpha_n y) = 0$, which gives $\alpha_n = n\pi$; where $n = 1, 2, 3, \ldots$ and the eigenfunctions

are

$$Y = Y_n = \cos(\alpha_n y) = \cos(n\pi y). \tag{4.12}$$

Now the (4.7) can be written as,

$$\frac{X''}{X} + k^2 + \alpha_n^2 = 0, \tag{4.13}$$

where $\eta_n = \sqrt{k^2 + \alpha_n^2}$ and then above equation reduces to

$$\frac{X''}{X} + \eta_n^2 = 0. \tag{4.14}$$

The solution of above equation for $X(x)$ is

$$X = C_7 e^{-i\eta_n x}, \tag{4.15}$$

where C_7 is an arbitrary constant. Now by the superposition principle in wave theory states that when two or more waves travel through the same medium at the same time, the resulting wave displacement at any point is equal to the algebraic sum of the displacements caused by each individual wave. So, substituting (4.12) and (4.15) into (4.6) and applying the superposition principle, the incident and reflection acoustic wave solutions for regions Φ_1, Φ_2 and Φ_3 are

$$\Phi_1 = \sum_{n=0}^{\infty} A_n \Phi_n e^{i\eta_n(x+L)} + \sum_{n=0}^{\infty} \delta_{n0} e^{i\eta_n(x+L)} \Phi_n, \tag{4.16}$$

$$\Phi_2 = \sum_{n=0}^{\infty} B_n \Phi_n e^{i\eta_n x} + \sum_{n=0}^{\infty} C_n \Phi_n e^{-i\eta_n x}, \tag{4.17}$$

$$\Phi_3 = \sum_{n=0}^{\infty} D_n \Phi_n e^{i\eta_n(x-L)}. \tag{4.18}$$

4.2.1 Symmetric Problem

To simplify the analysis of wave scattering through the double wire-mesh configuration, the problem is split into symmetric and anti-symmetric components. This technique leverages the mirror-like nature of the system to reduce complexity by

studying each symmetry class separately. In the symmetric case, the wave field behaves identically on both sides of the central plane, and the physical model is restricted to the left half of the waveguide (extending from $x = -\infty$) to $x = 0$). Here, a rigid wall at $x = 0$ ensures no wave passes through that boundary, while the wire mesh at $x = -L$ allows partial transmission and reflection. This reduction to a semi-infinite domain simplifies the boundary value problem and allows one to solve it using separation of variables techniques. This rectangular waveguide contain two regions of Φ_1^s and Φ_2^s. Again to solve this problem, we can use separation of variable method which gives the same eigenfunction (4.11) and eigenvalues. The geometrical configuration as shown in Figure 4.2.

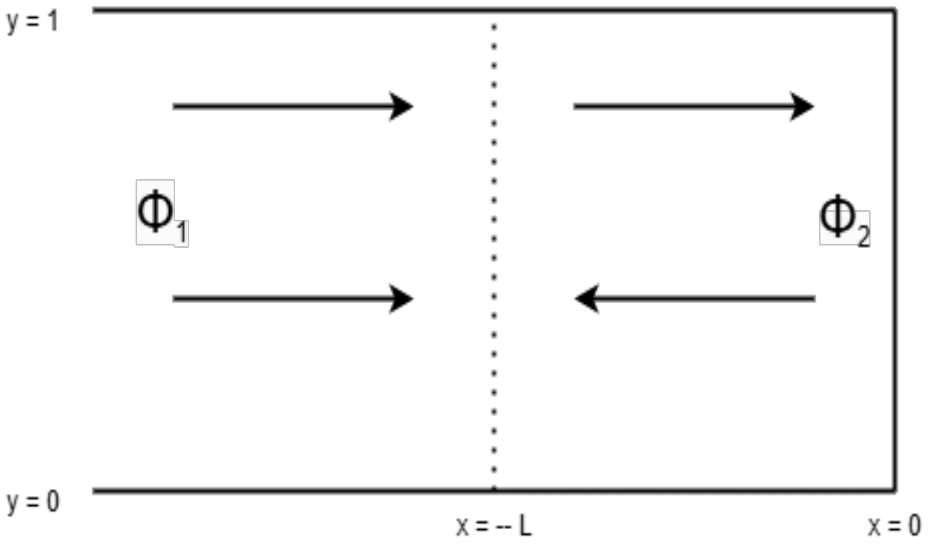

FIGURE 4.2: semi-infinite rectangular wave guide

In symmetric case incident and reflected acoustic wave equations after breakdown the configuration for region Φ_1^s and Φ_2^s are

$$\Phi_1^s = \sum_{n=0}^{\infty} A_n^s \Phi_n e^{-i\eta_n(x+L)} + \sum_{n=0}^{\infty} \delta_{n0} e^{i\eta_n(x+L)} \Phi_n, \tag{4.19}$$

$$\Phi_2^s = 2\sum_{n=0}^{\infty} B_n^s \Phi_n \cos(\eta_n x). \tag{4.20}$$

The following are the wire mesh boundary conditions for symmetric problem,

$$\frac{\partial \Phi_1^s}{\partial x} = \frac{\partial \Phi_2^s}{dx}, \quad x = -L, \tag{4.21}$$

$$\Phi_2^s - \Phi_1^s = \frac{iz}{k}\frac{\partial \Phi_2^s}{\partial x}, \quad x = -L. \tag{4.22}$$

By using the boundary condition (4.21) into (4.19) and (4.20), then we obtain

$$i\sum_{n=0}^{\infty}\delta_{n0}\Phi_n - i\sum_{n=0}^{\infty}A_n^s\Phi_n = -2\sum_{n=0}^{\infty}B_n^s \sin(\eta_n L)\Phi_n. \tag{4.23}$$

To make the orthogonality relation multiplying equation (4.23) with Φ_m and after integrating with respect to y from 0 to 1, we get

$$i\sum_{n=0}^{\infty}\delta_{n0}\int_0^1 \Phi_m\Phi_n dy - i\sum_{n=0}^{\infty}A_n^s\int_0^1 \Phi_m\Phi_n dy = 2\sum_{n=0}^{\infty}B_n^s \sin(\eta_n L)\int_0^1 \Phi_m\Phi_n dy. \tag{4.24}$$

Applying orthogonality relation in equation (4.24) and after simplification, we obtain

$$A_n^s = \delta_{n0} + 2iB_n^s \sin(\eta_n L). \tag{4.25}$$

Employing (4.19) and (4.20) into (4.22), we conclude that

$$2\sum_{n=0}^{\infty}B_n^s \cos(\eta_n L)\Phi_n - \sum_{n=0}^{\infty}\delta_{n0}\Phi_n - \sum_{n=0}^{\infty}A_n^s\Phi_n = \frac{iz}{k}[2\eta_n\sum_{n=0}^{\infty}B_n^s \sin(\eta_n L)\Phi_n]. \tag{4.26}$$

Multiplying equation (4.26) with Φ_m and after integrating with respect y from 0 to 1 yields to

$$\begin{aligned} 2\sum_{n=0}^{\infty}B_n^s \cos(\eta_n L)\int_0^1 \Phi_m\Phi_n dy - \sum_{n=0}^{\infty}\delta_{n0}\int_0^1 \Phi_m\Phi_n dy \\ -\sum_{n=0}^{\infty}A_n^s\int_0^1 \Phi_m\Phi_n dy = \frac{2i\eta_n z}{k}\sum_{n=0}^{\infty}B_n^s \sin(\eta_n L)\int_0^1 \Phi_m\Phi_n dy. \end{aligned} \tag{4.27}$$

Using orthogonality relation in equation (4.27) and after simplification, we get

$$2B_n^s \cos(\eta_n L) - B_n^s \sin(\eta_n L)\frac{2i\eta_n z}{k} = \delta_{n0} + A_n^s. \tag{4.28}$$

Using equation (4.25) into (4.28), then the B_n^s is

$$B_n^s = \frac{2k\delta_{n0}}{2k\cos(\eta_n L) - 2i\sin(\eta_n L)(k + \eta_n z)}. \tag{4.29}$$

Now using equation (4.29) into (4.25), we obtain

$$A_n^s = \delta_{n0}[\frac{2k\cos(\eta_n L) + 2i\sin(\eta_n L)(k - \eta_n z)}{2k\cos(\eta_n L) - 2i\sin(\eta_n L)(k + \eta_n z)}]. \tag{4.30}$$

4.2.2 Anti-Symmetric Problem

In the anti-symmetric problem, the configuration involves a semi-infinite rectangular waveguide extending in the negative x-direction, with a wire mesh boundary at $x = L$ and a soft boundary condition at $x = 0$.

Acoustic waves propagate within this semi-infinite waveguide, which is bounded horizontally between $y = 0$ to $y = 1$. The anti-symmetric case represents the part of the wave behavior that is odd with respect to the central plane of the original full-domain problem.

This simplified model allows for the analysis of how anti-symmetric wave components behave under such boundary conditions, which is essential for fully reconstructing the solution to the original full-domain scattering problem.

The geometrical configuration is shown in Figure 4.3.

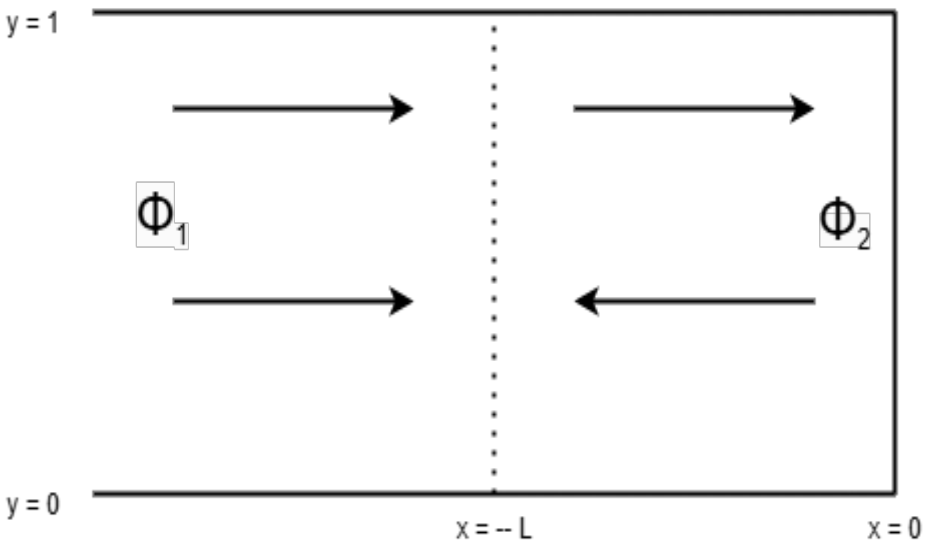

FIGURE 4.3: Infinite rectangular wave guide with two wire mesh

There is a anti-symmetric wave equation of incident and reflected transmission for region Φ^a_{1n} and Φ^a_{2n},

$$\Phi^a_{1n} = \sum_{n=0}^{\infty} A^a_n \Phi_n e^{-i\eta_n(x+L)} + \sum_{n=0}^{\infty} \delta_{n0} e^{i\eta_n(x+L)} \Phi_n, \tag{4.31}$$

$$\Phi^a_{2n} = 2i \sum_{n=0}^{\infty} B^a_n \Phi_n \sin(\eta_n x). \tag{4.32}$$

The wire-mesh boundary conditions for region Φ^a_{1n} and Φ^a_{2n} are,

$$\frac{\partial \Phi^a_{1n}}{\partial x} = \frac{\partial \Phi^a_{2n}}{\partial x}, \quad x = -L, \tag{4.33}$$

$$\Phi^a_{2n} - \Phi^a_{1n} = \frac{iz}{k} \frac{\partial \Phi^a_{2n}}{\partial x}, \quad x = -L. \tag{4.34}$$

By using the boundary condition (4.33) into (4.31) and (4.32) we obtain,

$$\sum_{n=0}^{\infty} \delta_{n0} \Phi_n - \sum_{n=0}^{\infty} A^a_n \Phi_n = 2 \sum_{n=0}^{\infty} B^a_n \cos(\eta_n L) \Phi_n. \tag{4.35}$$

The orthogonality relation enables the decomposition of complex fields—such as pressure, velocity, or displacement—into a series of independent modes (such as sine or cosine functions), allowing each mode to be analyzed separately. Now multiplying equation (4.35) with Φ_m and integrating from 0 to 1,

$$\sum_{n=0}^{\infty} \delta_{n0} \int_0^1 \Phi_m \Phi_n dy - \sum_{n=0}^{\infty} A^a_n \int_0^1 \Phi_m \Phi_n dy = 2 \sum_{n=0}^{\infty} B^a_n \cos(\eta_n L) \int_0^1 \Phi_m \Phi_n dy. \tag{4.36}$$

By using orthogonality relation in (4.36) and then after simplification we get,

$$A^a_n = \delta_{n0} - 2B^a_n \cos(\eta_n L). \tag{4.37}$$

Now again using equation (4.31) and (4.32) into (4.34) then we get,

$$-2i \sum_{n=0}^{\infty} B^a_n \sin(\eta_n L) \phi_n - \sum_{n=0}^{\infty} \delta_{n0} \phi_n - \sum_{n=0}^{\infty} A^a_n \phi_n = -\frac{2\eta_n z}{k} \sum_{n=0}^{\infty} B^a_n \cos(\eta_n L) \phi_n. \tag{4.38}$$

The eigenfunction orthogonal in nature in Φ_1 and Φ_2, To make the orthogonality relation multiplying equation (4.38) with Φ_m and integrating from 0 to 1, we get

the following solution

$$\begin{aligned} -2i\sum_{n=0}^{\infty} B_n^a \sin(\eta_n L)\int_0^1 \Phi_m \Phi_n dy - \sum_{n=0}^{\infty}\delta_{n0}\int_0^1 \Phi_m\Phi_n dy \\ -\sum_{n=0}^{\infty} A_n^a \int_0^1 \Phi_m\Phi_n dy = -\frac{2\eta_n z}{k}\sum_{n=0}^{\infty} B_n^a \cos(\eta_n L)\int_0^1 \Phi_m\Phi_n dy. \end{aligned} \tag{4.39}$$

Now using the orthogonality relation in (4.39) and after simplification we get,

$$-2iB_n^a \sin(\eta_n L) - \delta_{n0} - A_n^a = -\frac{2\eta_n z}{k} B_n^a \cos(\eta_n L). \tag{4.40}$$

Substituting (4.37) into (4.40) and we obtain,

$$B_n^a = \frac{2k\delta_{n0}}{2\cos(\eta_n L)(k+\eta_n z) - 2ik\sin(\eta_n L)}. \tag{4.41}$$

To find the value of A_n^a using (4.41) into (4.37) we obtain,

$$A_n^a = -\delta_{n0}[\frac{2\cos(\eta_n L)(k-\eta_n z) + 2ik\sin(\eta_n L)}{2\cos(\eta_n L)(k+(\eta_n)z)}]. \tag{4.42}$$

4.3 Numerical Results and Discussion

The symmetric and anti-symmetric problems are numerically solved by truncating the equations to N terms. This truncation is essential to reduce the system to a finite set of equations that can be handled using numerical techniques.

The resulting systems of equations are solved using PYTHON "NSolve" function, a robust tool for handling systems of nonlinear equations. To compute numerical solutions, specific values are assigned to the parameters in the equations, as outlined in reference d, density of air ρ, speed of sound in air c, frequency f, damping coefficient η and eigenvalue λ.

The selected parameter values are as follows: $c = 343.5$ m/s, $\rho = 1.63$ kg/m^3, $\eta = 0.005$ (damping Coefficient), $\lambda = n\pi$ and $f = 100$ Hz. These values are selected to represent a particular physical system, and the resulting numerical solutions provide insight into the system's behavior. For the numerical solution, the equations are truncated to include between 10 and 70 terms. This level of

truncation effectively captures the key dynamics of the system while maintaining a manageable computational cost. The results for the symmetric problem are presented in the Figure (4.4 - 4.8), where the real and imaginary parts of the velocities are plotted along y-axis at $x = -L$. The overlap of both velocity components confirms the validity of the truncated solution for the given parameter values. The result for the anti-symmetric problem plotted from Figure 4.9 to Figure 4.11. As expected from the symmetric configuration, both components are zero at this location. However, the pressure at this point is not zero, as illustrated in the corresponding pressure plot. In Figure 4.12 and Figure 4.13 graphs plotted the frequency against the amplitude A_0.

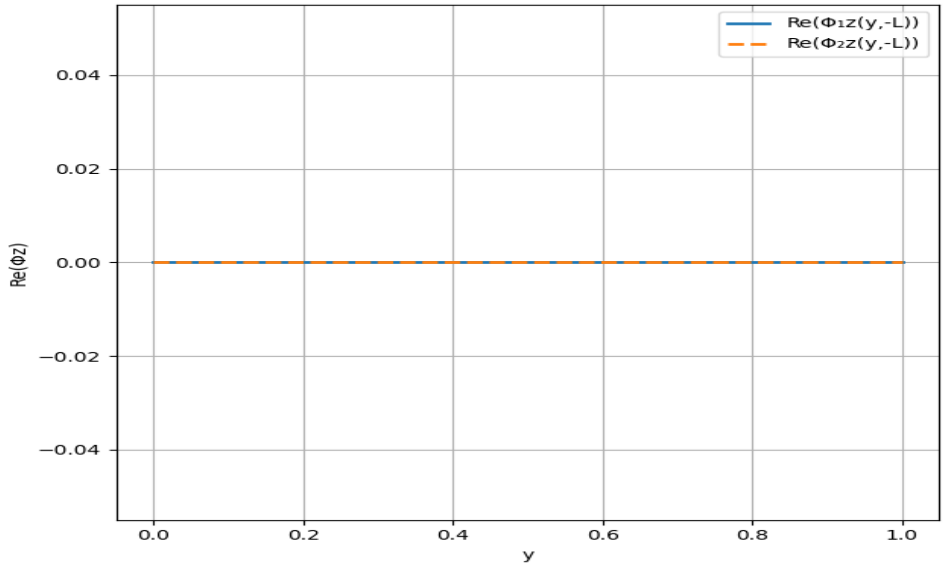

FIGURE 4.4: The real parts of the velocity, in symmetric case

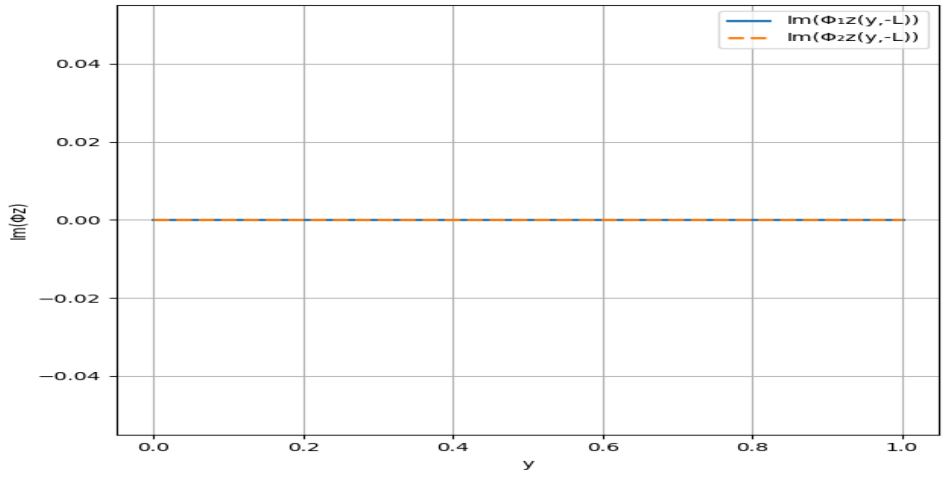

FIGURE 4.5: The imaginary parts of the velocity, in symmetric case

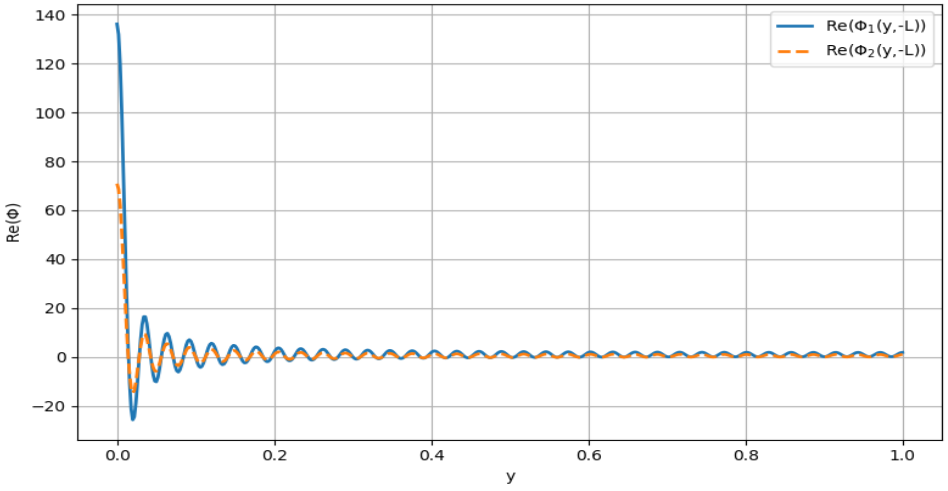

FIGURE 4.6: The real parts of the pressure, in symmetric case

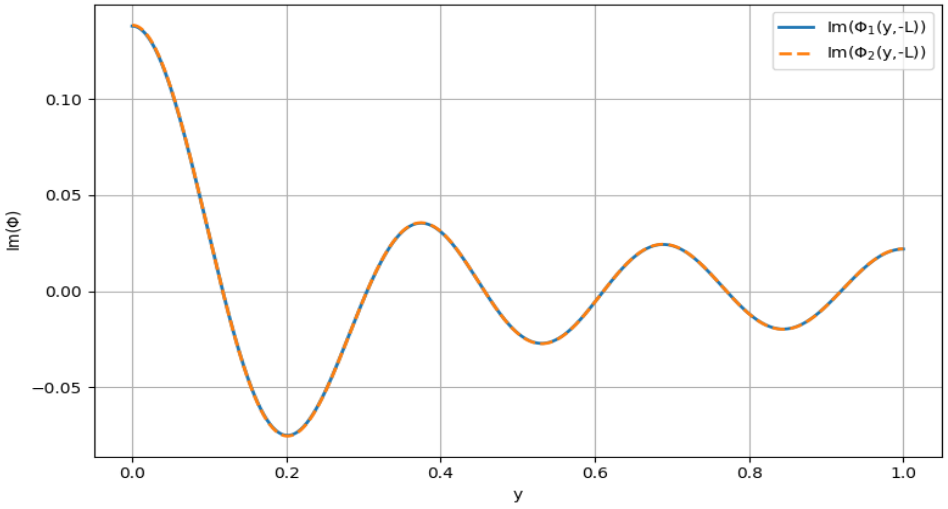

FIGURE 4.7: The imaginary parts of the pressure, in symmetric case

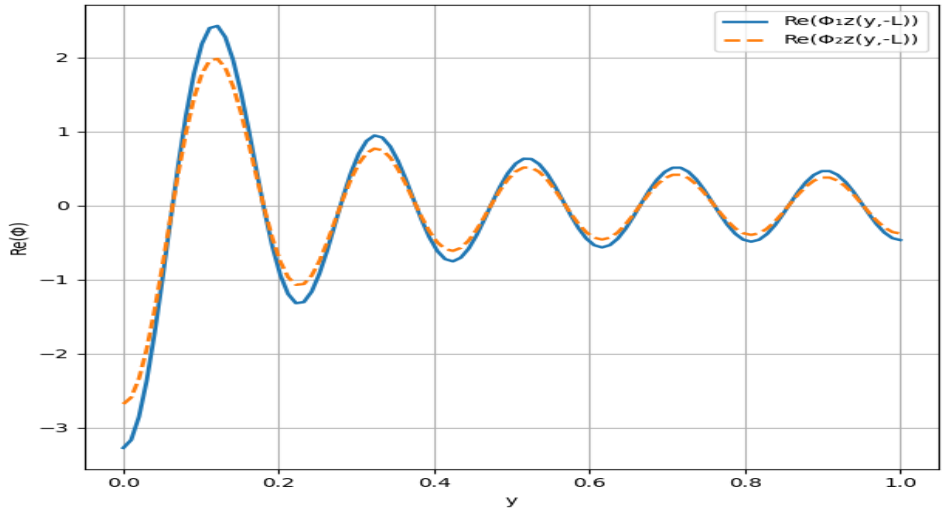

FIGURE 4.8: The real parts of the velocity, anti-symmetric case

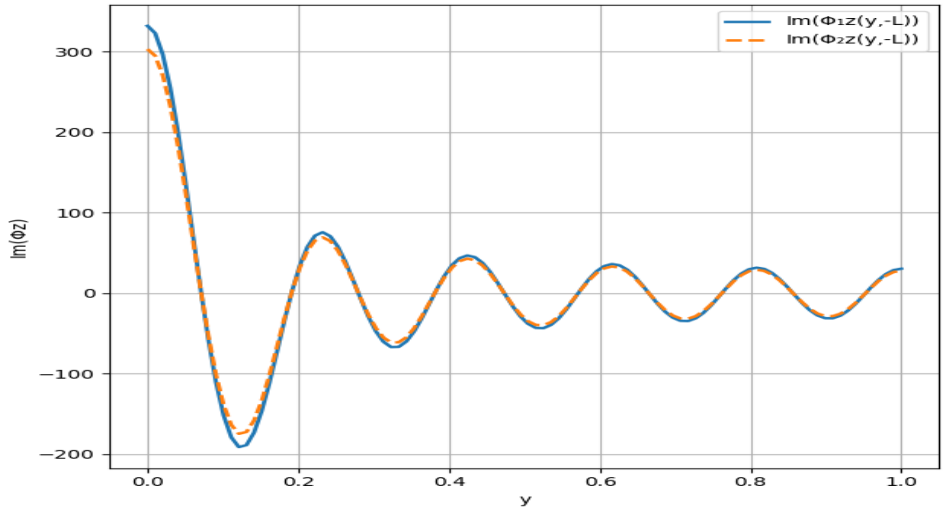

FIGURE 4.9: The imaginary parts of the velocity, in anti-symmetric case

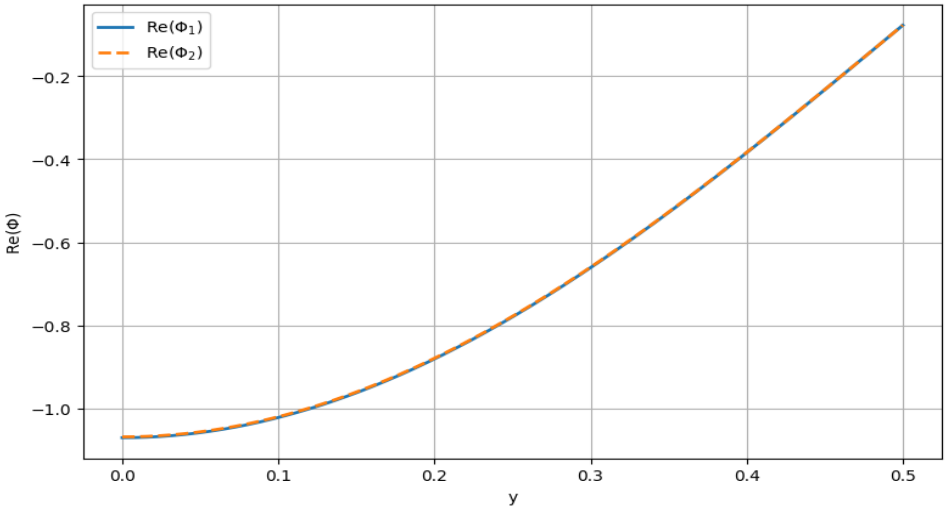

FIGURE 4.10: The real parts of the pressure, in anti-symmetric case

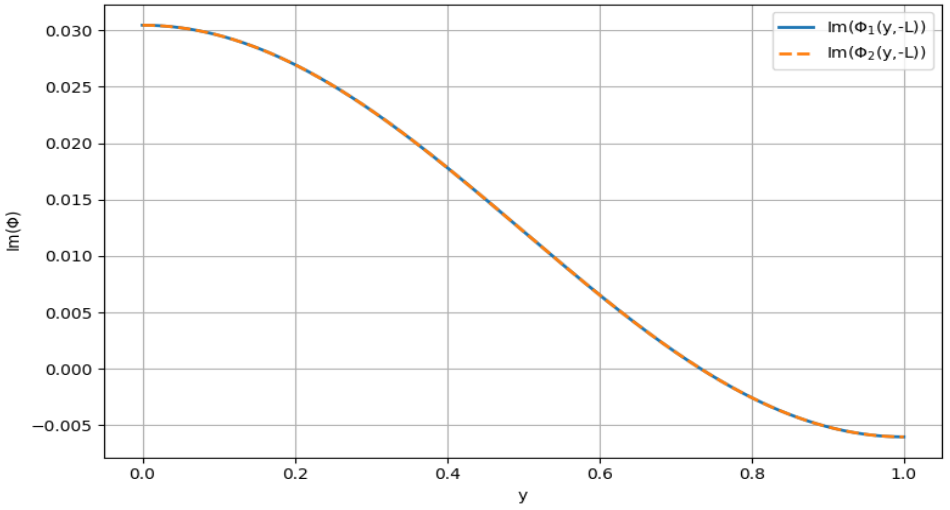

FIGURE 4.11: The imaginary parts of the pressure, in anti-symmetric case

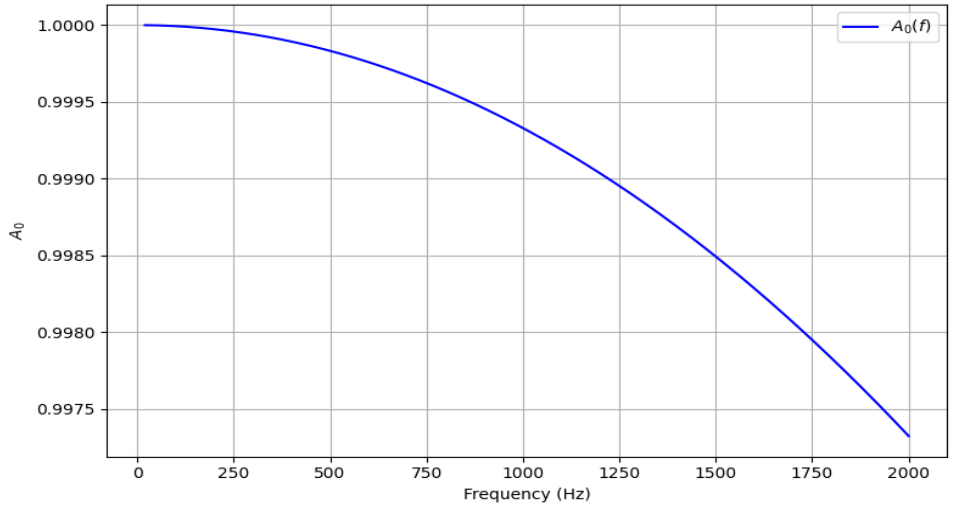

FIGURE 4.12: The frequency f against amplitude A_0, in symmetric case

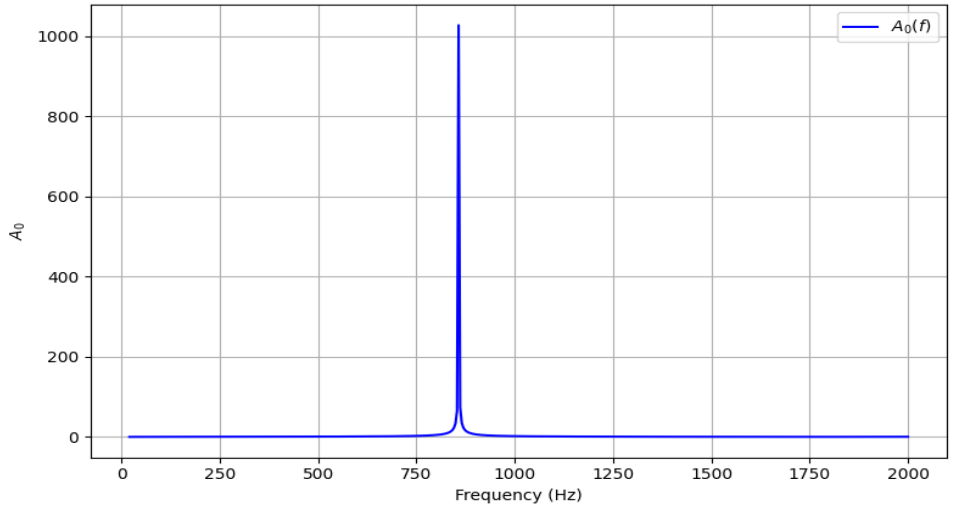

FIGURE 4.13: The frequency f against amplitude A_0, in in anti-symmetric case

Chapter 5

Summary and Conclusion

This research offers a thorough investigation into the reflection and transmission of acoustic waves within rectangular waveguides containing wire-mesh interfaces. The theoretical framework developed here delivers meaningful insights into the behavior of acoustic wave propagation and scattering when interacting with wire-mesh structures. By applying the separation of variables method, the study successfully tackles the complexities involved in modeling such intricate acoustic systems.

In this study, a two-dimensional wire-mesh is modeled within a rectangular waveguide. A fundamental mode is incident upon the wire-mesh, resulting in scattering due to its interaction with the mesh interface. To solve the governing boundary value problem, the method of separation of variables is employed. The resulting equations are truncated to a finite system, which is then solved to reveal the mode structure and propagation characteristics. As the frequency increases, additional modes are excited, emphasizing the significance of accounting for frequency-dependent effects on the system's dynamic behavior.

Chapter 4 focuses on the problem involving a wire-mesh backed by a rigid cavity. The modeling and analytical solutions for both symmetric and anti-symmetric mode problems are thoroughly discussed. The results show that the presence of a tensioned wire-mesh has a significant impact on wave behavior, influencing both transmission and reflection characteristics. Various configurations, including

cavity-backed and double wire-mesh setups, are examined, highlighting the critical influence of boundary conditions on wave interactions.

In present thesis the reflection and transmission of acoustic waves in rectangular waveguides with wire mesh interfaces is analyzed. First problem contains wire mesh interfaces at rectangular waveguide while the second problem include additionally the step-discontinuity. Further, it is found that the inclusion of step discontinuity affect the scattering waves in a rectangular waveguide.

The reflection and transmission of acoustic waves from expansion chamber in rectangular waveguides having wire mesh interfaces and step-discontinuities is discussed. For convenience the problem is divided into symmetric and anti-symmetric sub-problems. These problems are solved separately and then are combined by using mode matching conditions. It is observed that as the frequency increases, additional modes are excited; however, the velocity components continue to coincides, which they are confirming the validation of the truncated solutions. It is also found that the discontinuity and chamber length affect the reflecting and transmitting waves.

The outcomes of this study have significant implications for a range of engineering applications, such as noise control, architectural acoustics, and industrial sound management. The developed models can support the design of more effective noise barriers, acoustic filters, and resonators customized for specific needs. Future research may involve experimental validation of the theoretical results, as well as the exploration of more complex geometries and multi-layered membrane configurations to enhance and extend the current modeling approach.

In summary, this study enhances the understanding of acoustic wave interactions with tensioned wire-mesh interfaces, offering a strong foundation for future developments in noise control engineering and related disciplines.

The loss induced modal selection using a resistive wire mesh has numerous practical applications in wave physics and engineering. In microwave and optical waveguides, it helps suppress unwanted higher order modes while allowing the fundamental mode to pass efficiently resulting in cleaner signal transmission for

communication systems. In laser resonators resistive meshes act as mode selectors that maintain stable single mode operation essential for producing high quality, coherent beams in applications like precision measurement, spectroscopy, and material processing. In antenna arrays and radar systems, modal filtering with resistive wire meshes reduces interference and enhances directional control of radiation patterns. In acoustics, similar resistive meshes are used to manage standing waves in ducts and cavities, improving sound quality in auditoriums and lowering noise in ventilation systems. Furthermore, in plasma confinement and metamaterials, loss-induced modal control is applied to shape field distributions for energy localization, sensing, and wave absorption. Overall, this principle serves as a powerful tool across electromagnetics, optics, and acoustics to achieve selective mode propagation, improve performance, and minimize unwanted distortions.

Bibliography

[1] E. Dokumacı. *Duct acoustics: fundamentals and applications to mufflers and silencers*. Cambridge University Press, 2021.

[2] D. Zhang, X. Su, Y. Sun, C. Chen, and X. Sun. Mechanism analysis and experiment study for wire mesh-assisted ventilated acoustic metamaterials based on the acoustic analytical model and numerical acoustic-flow coupling model. *Journal of Vibration Engineering & Technologies*, 12(4):6649–6663, 2024.

[3] J.L. Young and J.R. Wait. Shielding properties of an ensemble of thin, infinitely long, parallel wires over a lossy half space. *IEEE transactions on electromagnetic compatibility*, 31(3):238–244, 1989.

[4] G. Ma and P. Sheng. Acoustic metamaterials: From local resonances to broad horizons. *Science advances*, 2(2):e1501595, 2016.

[5] W.C. Sabine. Collected papers on acoustics harvard university press. *Cambridge, MA.[Google Scholar]*, 1922.

[6] G.V. Norton and M.F. Werby. A numerical technique to describe acoustical scattering and propagation from an object in a waveguide. *Journal of applied physics*, 70(8):4101–4112, 1991.

[7] D. Tielbürger, S. Finette, and S. Wolf. Acoustic propagation through an internal wave field in a shallow water waveguide. *The Journal of the Acoustical Society of America*, 101(2):789–808, 1997.

[8] L.W. Cai, D.K. Dacol, D.C. Calvo, and G.J. Orris. Acoustical scattering by arrays of cylinders in waveguides. *The Journal of the Acoustical Society of America*, 122(3):1340–1351, 2007.

[9] A. Maurel, J.F. Mercier, and S. Félix. Wave propagation through penetrable scatterers in a waveguide and through a penetrable grating. *The Journal of the Acoustical Society of America*, 135(1):165–174, 2014.

[10] B.A. Plamenevskii, A.S. Poretskii, and O.V. Sarafanov. Mathematical scattering theory in quantum and acoustic waveguides. *Journal of Mathematical Sciences*, 262(3):329–357, 2022.

[11] R. Kirby. Modeling sound propagation in acoustic waveguides using a hybrid numerical method. *The Journal of the Acoustical Society of America*, 124(4):1930–1940, 2008.

[12] J.B. Lawrie. Analytic mode-matching for acoustic scattering in three dimensional waveguides with flexible walls: Application to a triangular duct. *Wave Motion*, 50(3):542–557, 2013.

[13] H. Afsar and M. M. Alam. Mode-matching analysis of flexural trifurcated waveguide with porosity effects. *Waves in Random and Complex Media*, pages 1–24, 2022.

[14] J.B. Lawrie, B. Nennig, and E. P.Debain. Analytic mode-matching for accurate handling of exceptional points in a lined acoustic waveguide. *Proceedings of the Royal Society A*, 478(2268):20220484, 2022.

[15] R.T. Muehleisen and D.C. Swanson. Modal coupling in acoustic waveguides: planar discontinuities. *Applied Acoustics*, 63(12):1375–1392, 2002.

[16] B. Tiryakioglu. Mode matching analysis of sound waves in an infinite pipe with perforated screen. *Acoustical Physics*, 66(6):580–586, 2020.

[17] H. Bilal and M. Afzal. On the extension of the mode-matching procedure for modeling a wave-bearing cavity. *Mathematics and Mechanics of Solids*, 27(2):348–367, 2022.

[18] J.B. Lawrie and M. Afzal. Acoustic scattering in a waveguide with a height discontinuity bridged by a membrane: a tailored galerkin approach. *Journal of Engineering Mathematics*, 105:99–115, 2017.

[19] A. Cummings and I.J. Chang. Sound attenuation of a finite length dissipative flow duct silencer with internal mean flow in the absorbent. *Journal of Sound and Vibration*, 127(1):1–17, 1988.

[20] B. Nennig, Y. Renou, J.P. Groby, and Y. Aurégan. A mode matching approach for modeling two dimensional porous grating with infinitely rigid or soft inclusions. *The Journal of the Acoustical Society of America*, 131(5):3841–3852, 2012.

[21] R. Kirby and J.B. Lawrie. A point collocation approach to modelling large dissipative silencers. *Journal of sound and vibration*, 286(1-2):313–339, 2005.

[22] M. Ayub, R. Nawaz, and A. Naeem. Diffraction of sound waves by a finite barrier in a moving fluid. *Journal of mathematical analysis and applications*, 349(1):245–258, 2009.

[23] L. Huang. Broadband sound reflection by plates covering side-branch cavities in a duct. *the Journal of the Acoustical Society of America*, 119(5):2628–2638, 2006.

[24] Y.S. Choy and L. Huang. Effect of flow on the drumlike silencer. *The Journal of the Acoustical Society of America*, 118(5):3077–3085, 2005.

[25] J.B. Lawrie. Comments on a class of orthogonality relations relevant to fluid-structure interaction. 2012.

[26] L. Huang. Modal analysis of a drumlike silencer. *the Journal of the Acoustical Society of America*, 112(5):2014–2025, 2002.

[27] A. Demır and A. Büyükaksoy. Transmission of sound waves in a cylindrical duct with an acoustically lined muffler. *International journal of engineering science*, 41(20):2411–2427, 2003.

[28] A. Iserles, A. Marthinsen, and S.P. Nørsett. On the implementation of the method of magnus series for linear differential equations. *BIT Numerical Mathematics*, 39:281–304, 1999.

[29] F. Casas and A. Iserles. Explicit magnus expansions for nonlinear equations. *Journal of Physics A: Mathematical and General*, 39(19):5445, 2006.

[30] K.T. Chen. Integration of paths, geometric invariants and a generalized baker-hausdorff formula. *Annals of Mathematics*, 65(1):163–178, 1957.

[31] R.W. Brockett. Volterra series and geometric control theory. *Automatica*, 12(2):167–176, 1976.

[32] V. Pagneux. Multimodal admittance method in waveguides and singularity behavior at high frequencies. *Journal of computational and applied mathematics*, 234(6):1834–1841, 2010.

[33] S. Félix and V. Pagneux. Sound propagation in rigid bends: A multimodal approach. *The Journal of the Acoustical Society of America*, 110(3):1329–1337, 2001.

[34] W.P. Bi, V. Pagneux, D. Lafarge, and Y. Aurégan. Sound propagation in non-uniform lined duct by the multimodal method. In *Proceedings of 10th International Conference on Sound and Vibration*, pages 3229–3236, 2003.

[35] J. Allard and N. Atalla. *Propagation of sound in porous media: modelling sound absorbing materials*. John Wiley & Sons, 2009.

[36] A.P. Mayer, V.V. Krylov, and A.M. Lomonosov. Guided acoustic waves propagating at surfaces, interfaces and edges. In *2011 IEEE International Ultrasonics Symposium*, pages 2046–2052. IEEE, 2011.

[37] E.B. Groth, T.G.R. Clarke, G. Schumacher da Silva, I. Iturrioz, and G. Lacidogna. The elastic wave propagation in rectangular waveguide structure: Determination of dispersion curves and their application in nondestructive techniques. *Applied Sciences*, 10(12):4401, 2020.

[38] S. Kuznetsova, Y. Aurégan, and V. Pagneux. Higher-order mode filtering by a resistive layer. *JASA Express Letters*, 3(10), 2023.

[39] Y. Ma, T. Liang, Y. Wang, Q. Zhang, and J. Hong. Experimental investigation of wave propagation characteristics in entangled metallic wire materials by acoustic emission. *Materials*, 16(13):4723, 2023.

[40] X. Qiu, X. Jing, L. Du, J. Yang, X. Sun, and X. Zhang. Nonlinear effect of wire mesh liners subjected to high sound pressure level. *AIAA Journal*, 60(9):5521–5532, 2022.

[41] S. Cao and S. Greenhalgh. Attenuating boundary conditions for numerical modeling of acoustic wave propagation. *Geophysics*, 63(1):231–243, 1998.

[42] I. Rudnick. The propagation of an acoustic wave along a boundary. *The Journal of the Acoustical Society of America*, 19(2):348–356, 1947.

[43] R.G. Keys. Absorbing boundary conditions for acoustic media. *Geophysics*, 50(6):892–902, 1985.

[44] J. Takekawa and H. Mikada. An absorbing boundary condition for acoustic-wave propagation using a mesh-free method. *Geophysics*, 81(4):T145–T154, 2016.

[45] Z. Wanxie and Z. Xiangxiang. Method of separation of variables and hamiltonian system. *Numerical Methods for Partial Differential Equations*, 9(1):63–75, 1993.

[46] R. Besancon. *The encyclopedia of physics*. Springer Science & Business Media, 2013.

[47] R.E. Collin. *Field theory of guided waves*. John Wiley & Sons, 1990.

[48] P. Photinos. Properties of waves. *The Physics of Sound Waves, 2053*, 2563:1–14, 2021.

[49] A.D. Pierce. *Acoustics: an introduction to its physical principles and applications*. Springer, 2019.

[50] P.M. Morse and K.U. Ingard. *Theoretical acoustics*. Princeton university press, 1986.

[51] M.A. Al-Gwaiz. *Sturm-Liouville theory and its applications*. Springer, 2008.

[52] W.A. Strauss. *Partial differential equations: An introduction*. John Wiley & Sons, 2007.

[53] S.J. Farlow. *Partial differential equations for scientists and engineers*. Courier Corporation, 1993.